Characterizing the Dynamics of the Type I interferon Response in SARS-CoV-2 Infection to Identify ISGs that Serve as Possible Antiviral Restriction Factors

Taylor Johnson

A thesis
submitted in partial fulfillment of the
requirements for the degree of

Master of Science

University of Washington
2021

Committee:
Michael Gale Jr.
Ram Savan

Program Authorized to Offer Degree:
Public Health Genetics

University of Washington

Abstract

Characterizing the Dynamics of the Type I Interferon Response in SARS-CoV-2 Infection to Identify ISGs that Serve as Possible Antiviral Restriction Factors

Taylor Johnson

Chair of the Supervisory Committee:

Michael Gale Jr.

Department of Immunology

Previous work has implicated a dysregulated IFN signaling pathway in severe cases of COVID-19 and found that treatment of IFNs in severe patients can decrease viral load. Here, we characterize the response to type I interferon to reveal the ISG signature of Calu-3 and ACE2/HSAEC1-KT cells after IFN-β treatment to identify specific ISGs as putative antiviral effector genes that may impart antiviral properties to inhibit SARS-CoV-2 replication. Treatment of IFN-β prior to SARS-CoV-2 infection regulated the expression of hundreds of ISGs resulting in early clearance of SARS-CoV-2 viral RNA. On the other hand, treatment of IFN-β after SARS-CoV-2 infection results in only minor changes in gene expression, owing to virus-directed blockades to the interferon signaling pathway and is not correlated with a decrease in SARS-CoV-2 RNA. Thus, early induction of the IFN signaling pathway indicates the ability for ISGs to quickly control SARS-CoV-2 infection whereas establishing the viral blockade to interferon signaling allows the virus to escape interferon actions later in the infection cycle. These studies show that after 24 hours of SARS-CoV-2 infection, the IFN signaling pathway is not able to overcome virus-controlled gene regulation, setting the stage for infection progression and disease. Thus, early ISG expression is essential for the control of SARS-CoV-2 infection.

Acknowledgements

I want to express my gratitude to my thesis chair, Michael Gale Jr., and my thesis advisory member, Ram Savan. The mentorship under Dr. Gale has been invaluable to my education and training. I would also like to thank members of the Gale lab, specifically Leanne Whitmore and Daniel Newhouse, who were instrumental in designing and carrying out the bioinformatic analyses. Lastly, I would like to acknowledge Akinobu Ota, a Visiting Scholar in the Department of Immunology. Dr. Ota designed and performed the experiment that generated the data set that I analyzed for this project. I greatly appreciate the support I have received throughout the completion of my thesis.

I. Introduction

Introduction to COVID-19

Coronavirus disease-2019 (COVID-19) was first reported in Wuhan, China in December 2019 and was declared a pandemic by the World Health Organization in March 2020. The causative pathogen of COVID-19, severe acute respiratory syndrome coronarivus-2 (SARS-CoV-2) is the third highly pathogenic coronavirus of global concern in recent decades. Individuals with COVID-19 present a wide range of clinical features from mild respiratory illness to severe acute respiratory disease syndrome (ARDS). Similar to severe acute respiratory syndrome coronavirus (SARS-CoV) and Middle East respiratory syndrome coronavirus (MERS-CoV), SARS-CoV-2 triggers the excessive production of proinflammatory cytokines known as a "cytokine storm" in severely ill patients (Huang et al., 2005; Huang et al., 2020; Mahallawi et al., 2018). These data suggest that SARS-CoV-2 may be dysregulating innate immune signaling pathways which can lead to tissue damage, multi-organ failure, and death (Ragab et al., 2020). Previous research has shown that SARS-CoV and MERS-CoV utilize a variety of mechanisms to evade the host immune response including reducing viral exposure to pathogen recognition receptors (PRRs) and antagonizing the interferon (IFN) pathway (Kindler et al., 2016; Moleaei et al., 2021). The exact role of the innate immune system in the pathogenesis of SARS-CoV-2 has yet to be fully understood. However, characterizing the host innate immune response to SARS-CoV-2 may elucidate antiviral drug targets.

Introduction to innate immunity

The innate immune system is the first line of defense against invading pathogens. During virus infection, PRRs detect conserved molecular patterns found in pathogens. These non-self

molecular motifs, known as pathogen associated molecular patterns (PAMPs), are essential to a pathogen's survival and accumulate within infected cells. PAMP recognition by PRRs activates an intracellular signaling cascade that alerts the host to a pathogenic infection and initiates the expression of genes whose products function to upregulate the innate immune response and inhibit viral replication. While the exact mechanism of PRR activation after SARS-CoV-2 infection is not yet fully understood, canonical viral PAMP sensing by PRRs, such as RIG-I and MDA5, activate the mitochondrial antiviral signaling protein (MAVS). MAVS then recruits the downstream kinases TBK1 and IKKi (Liu et al., 2015). These kinases phosphorylate and activate the transcription factors interferon regulatory factor (IRF) 3 and nuclear factor- κ B (NF- κ B) which in turn translocate to the nucleus to upregulate type I IFNs and other cytokines (McWhirter et al., 2003; Pomerantz and Baltimore, 1999). Type I IFNs consist of a family of cytokines that are essential to the innate immune response for their ability to mediate the expression of hundreds of genes with antiviral properties.

Introduction to Type I IFN signaling

After virus infection, PRR signaling leads to the production and secretion of type I IFNs and type III IFNs from an infected cell. While all cell types can produce and respond to type I IFNs, only a subset of tissues and cells can respond to type III IFNs. Type I IFNs are the largest class of IFNs and play a major role to control virus infection in vertebrate species. In mammals, the type I IFN family consists of IFN-α, IFN-β, IFN-ε, IFN-κ, and IFN-ω. IFN-α, and IFN-β are the most widely expressed type I IFNs and are well known for regulating the host innate immune response to viruses. The type I IFN receptor (IFNAR) is ubiquitously expressed and consists of the IFNAR1 and IFNAR2 subunits. Binding of the secreted type I IFN to the IFNAR of a

neighboring cell activates Janus kinase 1 (JAK1) and tyrosine kinase 2 (TYK2). Thereby, activated JAK1 and TYK2 phosphorylate signal transducer and activator of transcription 1 (STAT1) and STAT2. Phosphorylated STAT1 and STAT2 dimerize and join the interferon regulatory factor 9 (IRF9) to form the complex ISGF3. Activated ISGF3 translocates to the nucleus where it acts as transcription factor that binds to interferon-stimulated response elements (ISREs) upstream promoter regions of interferon-stimulated gene (ISGs) (Schindler et al., 2007). The IFN and JAK-STAT signaling pathway modulates the transcriptional regulation of hundreds of ISGs that collectively play a role in antiviral host immunity.

IFN responses by SARS-CoV-2

The response to SARS-CoV-2 infection has been defined by low levels of type I and III IFNs compared to other respiratory viruses (Blanco-Melo et al., 2020). A recent study found that 1 out of 5 critically ill COVID-19 patients had an impaired IFN-I response, including reduced ISG expression (Trouillet-Assant et al., 2020). Additionally, the same study was unable to detect IFN-β in mild to severe cases of COVID-19. Several studies have sought to address the molecular mechanisms underlying the IFN-signaling block after SARS-CoV-2 infection. The Nsp1, Nsp3, ORF3b, and ORF6 SARS-CoV-2 viral proteins have been implicated in its ability to inhibit type I IFN signaling and production (Lei et al., 2020; Konno et al., 2020; Shin et al., 2020; Thoms et al., 2020). However, only a minority of individuals infected with SARS-CoV-2 become severely ill suggesting the ability for most people to control infection through canonical innate immune pathways. Thus, IFN signaling likely has a critical role in the early control of SARS-CoV-2 and decreased severity of COVID-19, however the regulation of ISGs in response to SARS-CoV-2 is not well-defined. This study aims to address that knowledge gap.

Defining ISGs

For this research, the definition of an ISG is any gene that is responsive to IFN-β, including genes that are stimulated (upregulated) or repressed (downregulated) in response to IFN signaling. A substantial amount of research has been done to characterize ISGs and identify antiviral restriction factors. However, microarray and deep sequencing-based studies have yielded thousands of different ISGs (De Veer et al., 2001; Liu et al., 2018; Sarasin-Filipowicz et al., 2008). Additionally, ISG expression is highly complex and dependent on cell type, IFN dose, and type of infection. Previous work has identified the function of several ISGs known to antagonize viral replication including TRIM21, MX1, and RSAD2 (Crosse et al., 2017). However, the molecular functions of most ISGs in antiviral innate immunity remains widely unknown.

Characterizing the type I IFN response

In this study, we used functional genomics to define the ISG signature of two human airway epithelial cell lines treated with human recombinant IFN- β to better elucidate the role of IFN-β signaling during SARS-CoV-2 infection. After establishing baseline ISGs for each cell line, we interrogated their ISG signature under the following conditions: SARS-CoV-2 infection, IFN-β treatment before SARS-CoV-2 infection ("IFN- β pretreatment"), and IFN-β treatment after SARS-CoV-2 infection ("IFN-β posttreatment"). We investigated the ISG signatures of each treatment group to understand the ability of SARS-CoV-2 to dysregulate the IFN signaling pathway. Our study also reveals putative antiviral effector genes that evade viral suppression and may impart antiviral activity. Lastly, we found that treating Calu-3 and ACE2/HSAEC1-KT cells with IFN-β prior to SARS-CoV-2 infection results in early viral clearance and a down regulation of several proinflammatory cytokines during infection.

II. Materials and Methods.

Experimental design

The experiments reported in this study were performed in both Calu-3 and Human Small Airway Epithelial Cell (HSAEC1-KT) cell lines using an identical protocol. Cells were obtained from ATCC. Prior to the experiment, human ACE2 gene was stably introduced into parental HSAEC1-KT cells using a lentivirus system followed by cell sorting. SARS-CoV-2 Isolate USA-WA1/2020 was derived from BEI Resources. Viral infections were performed as previously described (Marchiano et al., 2020). For each treatment group, three biological replicates were harvested at each time point. Supernatant was collected from each sample for transcriptomic analysis. The following treatment groups are described below: IFN- β treatment, IFN- β pretreatment, and IFN- β posttreatment. Each treatment group has their own unique control that is matched according to time and IFN-β dose that is used as a comparator for bioinformatic analyses.

IFN-β treatment

Cells were first incubated for 24 hours at which point they were treated with either 10, 100, or 1,000 IU/mL of human recombinant IFN-β. IFN-β treatment signifies time zero. Samples were harvested at 6, 12, 24, and 48 hours post IFN-β treatment. To characterize the effect of IFN-β treatment on these samples, a control group was needed. For the IFN-β control group, cells were incubated for up to 72 hours. No treatment was provided, and samples were harvested at 24, 30, 36, 48, and 72 hours.

IFN-β pretreatment

Cells were incubated with 10, 100 or 1000 IU/mL of IFN-β for 24 hours. Three samples from each dose were harvested immediately after incubation which signifies time zero. The remaining samples were inoculated with SARS-CoV-2 at an MOI of 5. The cells were washed, given fresh medium, and placed back in the incubator. Samples were harvested at 6, 12, 24, and 48 hours post infection. To compare the effect of IFN-β pretreatment on SARS-CoV-2 ISG expression, an infection control group was needed. For the infection control, cells were incubated for 24 hours. Samples were harvested immediately after incubation which signifies time zero. The remaining cells were inoculated with SARS-CoV-2 at an MOI of 5. The cells were then washed and given fresh medium. These samples were placed back in the incubator and samples were collected at 6, 12, 24, and 48 hours post infection.

IFN-β posttreatment

Cells were inoculated with SARS-CoV-2 at an MOI of 5. Cells were then washed, given fresh medium, and incubated for 24 hours. After incubation, samples were treated with 10, 100, or 1000 IU/mL of IFN-β treatment which signifies time zero. Samples were collected at 6, 12, 24, and 48 hours after treatment. To compare the effect of IFN-posttreatment on SARS-CoV-2 ISG expression, an additional infected control group was needed. For this infection control, cells were first inoculated with SARS-CoV-2 at an MOI of 5. Cells were placed back in the incubator and samples were collected at 24, 30, 36, 48, and 72 hours post infection.

RNA sequencing

Bulk mRNA-seq data from Calu-3 cells were generated by constructing mRNA-seq libraries using the KAPA mRNA HyperPrep kit (Kapa Biosystems) and 250 ng of RNA. Bulk mRNA-seq data from ACE2/HSAEC1-KT cells were also generated by constructing mRNA-seq libraries using the mRNA HyperPrep kit and 180 ng of RNA. The RNA and resulting libraries were quality controlled and quantified using a 4200 TapeStation System (Agilent Technologies, Inc.) and a Qubit Fluorometer (Invitrogen). Libraries were sequenced on an Illumina NovaSeq using S2 v1.5 200 cycle flow cell which generates paired-end reads of 100 nucleotides. Each sample was sequenced to a minimum of 20 million mapped reads.

Preparation for differential expression analysis

Identical bioinformatic analyses were completed individually on the Calu-3 and ACE2/HSAEC1-KT samples using R (v 4.1.0)/Bioconductor (v 3.13) (Huber et al., 2015; R Core Team, 2021). Genes with less than 10 raw read counts averaged across all samples were removed. Raw read counts were transformed into log2-counts per million (logCPM) using the voom function (Law et al., 2014) in the R library *limma* (Ritchie et al., 2015). The logCPM were normalized using the trimmed means of means (TMM) method in the R library *edgeR* (Robinson and Oshlack, 2010). Principle component analysis (PCA) was performed on the $\log_2$(CPM) values of all expressed genes using the prcomp function in R (R Core Team, 2021). After visualization of the PCA plots, five samples from the Calu-3 cells did not cluster with their respective treatment groups and were removed from subsequent analyses (Fig S1) .

Differential expression analysis

To determine the significantly differentially expressed (DE) genes between each treatment group and its unique control, we used the *lm* function in the R library *stats* (R Core Team, 2021). Genes that had a false discovery rate (FDR)-adjusted $p \leq 0.01$ and absolute $\log_2(FC) > 2$ were considered significantly DE. The following DE comparisons were performed: IFN-β Treatment versus Control, Infected versus Control, IFN-β Pretreatment versus Infected Pretreatment Control, and IFN-β Posttreatment versus Infected Posttreatment Control. Within this list of ISGs (DE genes from the IFN-β Treatment versus Control), we identified genes that are differentially regulated by SARS-CoV-2 among the IFN-β pretreatment and IFN-β posttreatment DE genes. Differentially regulated ISGs from the IFN-β pretreatment and IFN-β posttreatment groups compared to their infected controls were defined as significantly differentially DE (DDE). Genes with a (FDR)-adjusted $p \leq 0.01$ and absolute $\log_2(FC) > 2$ were determined to be DDE.

Data visualization

Viral load data was plotted using ggplot2 (Wickham, 2016). For visualization of the number of DE genes between treatment groups, bar plots were also generated using ggplot2. Venny was used to create venn diagrams illustrating the number of overlapping DE genes in each treatment group (Oliveros, 2015). To create co-expression heatmaps, we first used the cutree function in the R library *stats* (R Core Team, 2021) to define co-expression gene modules (Langfelder et al., 2007). We then used the heatmap.2 function in the R library *gplots* (R Core Team, 2021) to perform hierarchical clustering of the co-expression modules. Gene set enrichment analysis (GSEA) was conducted using the Over-Representation Analysis (ORA) method from the R library *WebGestaltR* (Liao et al., 2019). Pathway enrichment and upstream regulator analyses

were performed using Ingenuity Pathway Analysis (IPA) (Kramer et al., 2013). Interaction networks were built using Cytoscape software (Shannon et al., 2003).

III. Results

Baseline ISGs

To characterize the ISG signature of IFN-β treatment, we compared the gene expression response of IFN-β treated cells compared to their control. We identified genes that were statistically significantly DE at any IFN-β treated time point compared to the control in any of the three IFN-β doses (10, 100, 1000 IU/mL). Using bioinformatic analyses and linear modeling, we identified 652 and 2,766 DE genes in the Calu-3 cells and ACE2/HSAEC1-KT cells, respectively. These gene lists represent the baseline ISGs for each cell type (S2 Table and S3 Table). Among the ISGs identified, 383 genes were DE in both cell types (S4 Table). Differential regulation occurs immediately after IFN-β treatment and persists for at least 48 hours (Fig 1A). In both cell types, the number of DE genes increases as time elapses and the IFN-β dose increases. To further investigate these ISGs, we ran GSEA on co-expression modules from the heatmap. For both cell types, the upregulated clusters are mainly associated with innate immune signaling including IFN signaling, response to virus, and cytokine production. In contrast, the downregulated gene clusters are mainly associated with cell cycle progression and translational initiation.

ISG network analysis

To understand the molecular mechanisms driving the response to IFN-β, we used IPA to interrogate our list of ISGs to identify the top upstream regulators in each heatmap cluster from Figure 1. Among the upregulated clusters, the top transcription factors that best explain the

observed gene expression changes include NONO, STAT1, NKX2-3, and IRF3 (S1 Table). To identify the interaction between the transcription factors and ISGs, we built interaction networks around NONO, STAT1, NKX2-3, and IRF3 using the DE genes from each cluster (Fig 2 and Fig 3). While STAT1 and IRF3 are well known for their role in antiviral immunity, the role of NONO and NKX2-3 in the IFN signaling pathway has yet to be elucidated. The interaction networks built around these transcription factors demonstrate a considerable amount of crosstalk between NONO, NKX2-3, STAT1, and IRF3 in IFN signaling (Fig 2 and Fig 3).

ISG signature of SARS-CoV-2

After identifying genes that are statistically significantly DE in response to IFN-β treatment (ISGs), we wanted to visualize their gene expression signature after SARS-CoV-2 infection. To do this, we first obtained the $\log_2$FC gene expression values in the infected group compared to baseline. This gene signature was defined as the viral induced gene signature. We then removed all viral induced genes that were not from the original ISG list. We now had the viral induced gene expression values of the ISGs. In Figure 1, we saw immediate changes in gene expression of ISGs after IFN-β treatment. However, the same set of genes have a delayed response after SARS-CoV-2 infection (Fig 4). SARS-CoV-2 appears to elicit IFN signaling by 24 hours which is when we see a stark change in the gene expression profile of the ISGs. GSEA of the co-expression modules indicated that upregulated clusters were associated with defense responses to other organisms and IFN-gamma responses in both cell lines. The downregulated clusters were associated with protein localization to the ER and cell cycle progression in the Calu-3 and the ACE2/HSAEC1-KT cells, respectively (Fig 4).

IFN-β pretreatment

In order to understand the effect of IFN-β pretreatment on SARS-CoV-2 induced gene expression, we first identified genes that are DE between the IFN-β pretreatment group and its infected control. The 2,995 DE genes in the Calu-3 cells (Table S5) and 5,830 DE genes in the ˙ACE2/HSAEC1-KT cells (Table S6) were defined as genes differentially regulated by the IFN-β pretreatment. Next, we wanted to determine the effect of the IFN-β pretreatment on ISG activity in response to SARS-CoV-2 infection. To do this, we identified genes showing significant variation in baseline ISG expression compared to the effect of IFN-β treatment before infection. The genes that were significantly differentially DE across the time course in any of the three IFN-β doses were defined as DDE genes. The 2,911 DDE genes in the Calu-3 cells (Table S7) and 6,398 DDE genes (Table S8) in the ACE2/HSAEC1-KT cells represent genes whose response to IFN-β treatment is differentially regulated by treatment with IFN-β before SARS-CoV-2 infection (Fig 5). In the Calu-3 and ACE2/HSAEC1-KT cells, the genes that are significantly upregulated in response to IFN-β treatment (ISGs) are initially upregulated in the IFN-β pretreatment compared to infection. However, by 24 hours, the same clusters of ISGs are downregulated in the IFN-β pretreatment group compared to infection alone (Clusters 1-3). Genes within these clusters were associated with defense response to other organisms, IFN signaling, and receptor ligand activity. In contrast, genes that are downregulated by IFN-β treatment are upregulated in the IFN-β pretreatment group after 24 hours of infection in both cell types (Cluster 4). Genes within these clusters were associated with drug metabolism and mitotic cell cycle phase transition.

IFN-β posttreatment

To elucidate the effect of IFN-β posttreatment on SARS-CoV-2 induced gene expression, we first identified genes that are DE between the IFN-β posttreatment group and its infected control. The 65 DE genes in the Cau-3 cells (Table S9) and 15 DE genes in the ACE2/HSAEC1-KT cells (Table S10) were defined as genes responding to virus that are differentially regulated by treatment of IFN-β post infection. This analysis suggests that SARS-CoV-2 infection is controlling gene expression by the time the cells were treated with IFN-β as indicated by the minimal differences seen in gene expression levels. Next, we wanted to determine the effect of IFN-β posttreatment on ISG activity after SARS-CoV-2 infection. To do this, we identified genes showing significant variation between the baseline ISG expression compared to the effect of IFN-β treatment after infection. The genes that were significantly differentially DE across the time course in any of the three IFN-β doses were defined as DDE genes. The 810 DDE genes in the Calu-3 cells (Table S11) and 2,097 DDE genes in the ACE2/HSAEC1-KT cells (Table S12) represent genes whose response to IFN-β treatment is differentially regulated when treated with IFN-β after SARS-CoV-2 infection (Fig 6). All three clusters in the Calu-3 cells show a remarkable dysregulation of genes responsive to IFN-β. There is a slight dose response relationship at the 30-hour time point (directly after IFN-β posttreatment) where we see an increase in the upregulation of ISGs as IFN-β dose increases (Cluster 1 and 2). However, by 36 hours, IFN signaling appears to again be dysregulated. In the ACE2/HSAEC1-KT cells, the gene expression signature of ISGs next to IFN-β posttreatment illustrates a stark contrast. Genes upregulated and downregulated by IFN-β treatment (Clusters 1-4) show little variation in their gene expression profile in the IFN-β posttreatment group compared to its infected control.

IFN-β pretreatment anti-viral effectors

After establishing ISGs and characterizing their gene signature across the pretreatment and posttreatment conditions, we next wanted to identify potential antiviral effector genes. For our purposes, anti-viral effectors are defined as ISGs that retain their expression in the presence of infection and may impart antiviral actions to suppress viral RNA replication. For the IFN-β pretreatment group, an antiviral effector was thought to be initially upregulated by the IFN-β treatment and retain expression once infected with SARS-CoV-2. To identify these genes in the pretreatment samples, we started with the genes that were DE when treated with IFN-β before infection compared to infection. These are the genes responding to virus that are differentially regulated by treatment of IFN-β prior to infection. Among these DE genes, we identified genes that were upregulated (log_2(FC) >2) after being treated with IFN-β for 24 hours compared to control. We further interrogated this list of DE genes by defining genes that retained expression (log_2(FC) >2) 48 hours post infection in any of the three doses. These genes were considered potential antiviral effectors for their ability to escape viral suppression for 48 hours at which point gene expression is widely regulated by the virus. This analysis elucidated 23 genes in the Calu-3 cells (Table 1) and 118 genes in the ACE2/HSAEC1-KT (Table 2) that escape viral suppression. None of the putative antiviral genes identified were seen in both the Calu-3 and ACE2/HSAEC1-KT IFN-β pretreatment samples.

IFN-β posttreatment anti-viral effectors

To establish antiviral effectors from the IFN-β posttreatment samples, we identified ISGs that can be induced by IFN-β after 24 hours of SARS-CoV-2 infection. These genes are putative

antiviral effector genes for their ability to be activated by IFN and overcome SARS-CoV-2 regulated gene expression. To identify these genes in the posttreatment samples, we started with the genes that were DE when treated with IFN-β after infection compared to infection. These are the genes that are responding to virus that are differentially regulated when treated with IFN-β post infection. Among these genes, we identified genes that can be activated 72 hours after infection ($\log_2$(FC) >0) while being treated with IFN-β. These genes are putative antiviral effectors for their ability to become activated by IFN-β treatment after SARS-CoV-2 has already begun to dysregulate IFN signaling. This analysis elucidated 33 genes in the Calu-3 cells (Table 3) and 14 genes in the ACE2/HSAEC1-KT cells (Table 4) that are still inducible by IFN-β 72 hours post SARS-CoV-2 infection. Only two putative antiviral effectors, GMPR and CXCL10, were identified in both the Calu-3 and ACE2/HSAEC1-KT IFN-β posttreatment samples.

IV. Discussion.

This study provides novel insights into the IFN signaling pathway in response to SARS-CoV-2 infection. The hyperinflammatory response and cytokine storm seen in severely ill COVID-19 patients has drawn attention to the IFN signaling pathway of the innate immune response. Previous work has reviewed the role of IFNs during SARS-CoV-2 infection (Shibabaw et al., 2020), but ISG regulation in response to IFN signaling is not fully understood. Recently, IFNs have been evaluated as treatments to COVID-19 due to their inherent ability to induce hundreds of ISGs that collectively inhibit viral replication. The use of IFNs to treat COVID-19 patients has resulted in decreased viral load, inflammatory markers, and mortality (Davoudi-Monfared et al., 2020; Zhou et al., 2020). This study uses bioinformatic analyses to characterize the gene

signature of IFN signaling during SARS-CoV-2 infection and treatment of IFN-β on two human epithelial cell lines.

DE analysis of IFN-β treatment compared to control revealed thousands of genes that are differentially regulated in response to IFN-β in Calu-3 and ACE2/HSAEC1-KT cells. While the ACE2/HSAEC1-KT cells had more DE genes, both cell types had remarkably similar gene expression signatures (Fig 1). We found that IFN-β treatment results in immediate changes in ISG expression and persists until at least 48 hours post treatment. Additionally, we show that increasing doses of IFN-β is correlated with an increase in DE gene expression. The ISG signature in both cell types include the upregulation of genes associated with IFN signaling and the downregulation of genes associated with cell cycle progression and translation.

We further characterized the functional modules identified from the cluster analysis by building networks around common upstream regulators from our ISG list. Among the top upstream regulators for each cluster, STAT1, IRF3, NONO, and NKX2-3 were of interest for building the interaction networks. STAT1 and IRF3 are well known for their role in inducing the IFN signaling pathway. However, the transcription factors, NONO and NKX2-3 have not been definitively linked to IFN signaling during RNA viral infections. The gene NONO (non-POU domain containing octamer binding) encodes an RNA-binding protein involved in transcriptional regulation and RNA splicing. NONO has been linked to the negative regulation of HIV infection in CD4+T cells, but little is known about the mechanism behind this interaction (St. Gelais et al., 2015). NKX2-3 (NK2 Homeobox 3) encodes a homeodomain-containing transcription factor that regulates B-cell receptor signaling and is linked to B-cell lymphoma (Robles et al., 2016).

Among the upstream regulators used as central nodes, STAT1 was DE between IFN-β treatment and the control in both the Calu-3 and ACE2/HSAEC1-KT cells and remained activated throughout the time course. The interaction networks collectively demonstrate the upregulation of STAT1 signaling in response to IFN-β treatment. Recent evidence that SARS-CoV-2 suppresses the phosphorylation and nuclear localization of STAT1 (Mu et al., 2020) was not validated in this analysis. STAT1 was also significantly upregulated by 24 hours in both cell types after SARS-CoV-2 infection (S1 Table). NONO was only DE in the ACE2/HSAEC1-KT cells (S1 Table) and exhibited decreasing expression in response to IFN-β treatment throughout the time course. While IRF3 and NKX2-3 were not themselves statistically significant in our dataset (S1 Table), the interaction networks indicate substantial crosstalk between the transcription factors and their targets (Fig 2 and Fig 3). NONO and NKX2-3 appear to play an important role the regulation of ISGs, despite the fact that NONO is gradually downregulated, and NKX2-3 is not differentially regulated by IFN. The role of NONO and NKX2-3 in the activation of ISGs warrants further exploration.

Our analysis of ISGs in response to SARS-CoV-2 infection shows that IFN signaling is delayed until approximately 24 hours post-infection (Fig 4). Next, we analyzed the effect of IFN-β treatment before infection and post infection on SARS-CoV-2 induced ISG expression. Our analysis of the IFN-β pretreatment DDE genes shows that genes initially upregulated by IFN-β treatment before infection are downregulated in the pretreatment samples compared to infected samples from 24-48 hours. This may be evidence that the the virus is mitigating IFN signaling around 24 hours post infection, which correlates with the viral induced gene expression signature initiated at the same timepoint (Fig 3). Viral load data demonstrates a dramatic decrease in viral

replication in cells that are treated with IFN-β treatment before infection (Fig 7). While IFN signaling appears to be mitigated in the pretreatment Calu-3 and ACE2/HSAEC1-KT samples by 48 hours post infection, the initial upregulation appears to be sufficient in controlling viral replication. Furthermore, genes associated with the cytokine storm phenotype seen in severely ill patients including IL-6, TNF-α, and IL-8 (Darif et al., 2021) demonstrate this same expression profile and are downregulated compared to infection starting at 24 hours post infection. We hypothesize that IFN-β treatment prior to infection may impart protection against severe disease by restricting the production of proinflammatory cytokines associated with COVID-19 disease progression. Additional studies evaluating this relationship may provide insights into using IFN-β treatment as a preventative measure in individuals at high risk for severe illness.

To identify genes that may impart antiviral activity against SARS-CoV-2, we interrogated the genes that were differentially regulated by IFN-β pretreatment compared to infection. Among the thousands of DE genes in the IFN-β pretreatment samples, we identified 22 and 118 potential antiviral effector genes in the Calu-3 cells and ACE2/HSAEC1-KT cells, respectively (Table 1 and Table 2). These ISGs show promising capabilities to be induced by IFN-β and maintain their expression in the presence of SARS-CoV-2 infection for up to 48 hours. Several genes identified between the two cell types are known to be induced by IFN and antagonize viral replication, including MX1 and MX2, OAS, TRIM22, GBP2, and MOV10 and should be looked at closely in additional studies.

While SARS-CoV-2 patients have shown to be responsive to IFN-β treatment after infection, our analysis provided evidence that *in vitro*, Calu-3 and ACE2/HSAEC1-KT cells are insensitive to

IFN-β treatment post infection. Cells treated with IFN-β post infection showed increasing viral replication for up to 30 hours post treatment in the ACE2/HSAEC1-KT samples and up to 36 hours post treatment in the Calu-3 samples (Fig 7). Unlike the pretreatment analysis, this suggests that IFN-β treatment is unable to inhibit SARS-CoV-2 replication after 24 hours of infection (when IFN-β treatment was given). This finding is supported by the relatively small handful of genes that are differentially regulated by IFN-β treatment post infection compared to infection. The DDE analysis further illustrated the inability to enhance IFN signaling after infection (Fig 6). A small subset of ISGs from Cluster 1 in the ACE2/HSAEC1-KT cells exhibit a slight increase in expression at the highest IFN dose immediately following treatment, but by 12 hours this gene signature is lost (Fig 6). Taken together, this data indicates that overall, IFN-β treatment post infection is unable to enhance IFN signaling and control viral replication.

Among the 65 genes in the Calu-3s and 15 genes in the ACE2/HSAEC1-KT cells that were found to be statistically significantly regulated by IFN-β treatment post infection, we identified 33 and 14 potential antiviral effector genes, respectively (Table 3 and Table 4). These genes were able to escape viral suppression and maintain positive gene expression signatures ($\log_2$(FC) >0) for 48 hours post treatment (72 hours post infection). Additional research is needed to characterize the antiviral properties imparted by these genes that allow them to escape viral suppression. Furthermore, genes identified to have antiviral properties can be defined as potent anti-SARS-CoV-2 restriction factors and investigated as potential immunotherapeutic targets.

This study had several limitations. The experimental design of the study did not include time points beyond 48 hours in the IFN-β treatment samples. For this reason, we cannot conclusively

determine if IFN signaling in the pretreatment group is suppressed by the virus beyond 48 hours post treatment or if the down regulation is occurring as a result of IFN-β treatment wearing off. However, the effects of the IFN-β treatment on viral load in the pretreatment samples suggests that early clearance of the virus is the reason for a downregulated ISG signature in the later time points. Additionally, five outliers were removed from the Calu-3 cells to limit variability among the samples which may have increased the risk for spurious associations in those treatment groups.

V. Conclusion

It is critical to understand the innate immune response to SARS-CoV-2 in order to identify therapeutic targets. The hyperimmune response seen in severe cases of COVID-19 suggest the ability of SARS-CoV-2 to dysregulate the innate immune response. Since IFN signaling is the first line of defense against RNA viruses, understanding the molecular mechanisms by which SARS-CoV-2 can be targeted by ISGs could be crucial in combating this pandemic. Here, we define genes that are induced by IFN-β in two cell types from the lower respiratory tract that overall, show similar gene expression signatures. We found that early induction of the IFN signaling pathway prior to infection in Calu-3 and ACE2/HSAEC1-KT cells lead to early clearance of SARS-CoV-2 and subsequent downregulation of IFN signaling that may protect against the cytokine storm seen in severe cases of COVID-19. We also found that Calu-3 and ACE2/HSAEC1-KT cells establish a viral blockade that inhibits IFN signaling that allows the virus to escape IFN signaling later in infection. Thus, cells treated with IFN-β post-infection had a delayed ability to clear SARS-CoV-2 RNA and the IFN signaling pathway was not able to overcome virus-controlled gene regulation. Our results indicate the importance of early induction

of IFN signaling to control SARS-CoV-2 infection. This result seems to contradict reports that IFNs used to treat both SARS (Loutfy et al., 2003) and COVID-19 (Zhou et al., 2020) *in vitro* are effective. Therefore, the putative antiviral effector genes that we identified may be the key to understanding the relationship between ISG regulation and ability of IFN signaling to suppress SARS-CoV-2 infection.

References.

1. Belgnaoui, S. M., Paz, S., & Hiscott, J. (2011). Orchestrating the Interferon antiviral response through the Mitochondrial ANTIVIRAL Signaling (MAVS) adapter. *Current Opinion in Immunology*, *23*(5), 564–572. https://doi.org/10.1016/j.coi.2011.08.001

2. Blanco-Melo, D., Nilsson-Payant, B. E., Liu, W.-C., Uhl, S., Hoagland, D., Møller, R., Jordan, T. X., Oishi, K., Panis, M., Sachs, D., Wang, T. T., Schwartz, R. E., Lim, J. K., Albrecht, R. A., & tenOever, B. R. (2020). Imbalanced host response to sars-cov-2 drives development of covid-19. *Cell*, *181*(5). https://doi.org/10.1016/j.cell.2020.04.026

3. Crosse, K. M., Monson, E. A., Beard, M. R., & Helbig, K. J. (2017). Interferon-Stimulated genes as Enhancers of Antiviral innate Immune Signaling. *Journal of Innate Immunity*, *10*(2), 85–93. https://doi.org/10.1159/000484258

4. Darif, D., Hammi, I., Kihel, A., El Idrissi Saik, I., Guessous, F., & Akarid, K. (2021). The pro-inflammatory cytokines in Covid-19 pathogenesis: What goes wrong? *Microbial Pathogenesis*, *153*, 104799. https://doi.org/10.1016/j.micpath.2021.104799

5. Davoudi-Monfared, E., Rahmani, H., Khalili, H., Hajiabdolbaghi, M., Salehi, M., Abbasian, L., Kazemzadeh, H., & Yekaninejad, M. S. (2020). A randomized clinical trial of the efficacy and safety of interferon β-1a in treatment of severe covid-19. *Antimicrobial Agents and Chemotherapy*, *64*(9). https://doi.org/10.1128/aac.01061-20

6. De Veer, M. J., Holko, M., Frevel, M., Walker, E., Der, S., Paranjape, J. M., Silverman, R. H., & Williams, B. R. G. (2001, June 1). *Functional classification of interferon-stimulated genes identified using microarrays*. JLB. https://jlb.onlinelibrary.wiley.com/doi/full/10.1189/jlb.69.6.912.

7. Huang, C., Wang, Y., Li, X., Ren, L., Zhao, J., Hu, Y., Zhang, L., Fan, G., Xu, J., Gu, X., Cheng, Z., Yu, T., Xia, J., Wei, Y., Wu, W., Xie, X., Yin, W., Li, H., Liu, M., … Cao, B. (2020). Clinical features of patients infected With 2019 novel coronavirus IN WUHAN, CHINA. *The Lancet*, *395*(10223), 497–506. https://doi.org/10.1016/s0140-6736(20)30183-5

8. Huang, K.-J., Su, I.-J., Theron, M., Wu, Y.-C., Lai, S.-K., Liu, C.-C., & Lei, H.-Y. (2004). An interferon-gamma-related cytokine storm in SARS patients. *Journal of Medical Virology*, *75*(2), 185–194. https://doi.org/10.1002/jmv.20255

9. Huber, W., Carey, V. J., Gentleman, R., Anders, S., Carlson, M., Carvalho, B. S., Bravo, H. C., Davis, S., Gatto, L., Girke, T., Gottardo, R., Hahne, F., Hansen, K. D., Irizarry, R. A., Lawrence, M., Love, M. I., MacDonald, J., Obenchain, V., Oleś, A. K., … Morgan, M. (2015). Orchestrating high-throughput genomic analysis WITH BIOCONDUCTOR. *Nature Methods*, *12*(2), 115–121. https://doi.org/10.1038/nmeth.3252

10. Kindler, E., Thiel, V., & Weber, F. (2016). Interaction of SARS and MERS CORONAVIRUSES with the Antiviral interferon response. *Coronaviruses*, 219–243. https://doi.org/10.1016/bs.aivir.2016.08.006

11. Konno, Y., Kimura, I., Uriu, K., Fukushi, M., Irie, T., Koyanagi, Y., Sauter, D., Gifford, R. J., Nakagawa, S., & Sato, K. (2020). SARS-CoV-2 ORF3b is a potent interferon antagonist whose activity is increased by a naturally occurring elongation variant. *Cell Reports*, *32*(12), 108185. https://doi.org/10.1016/j.celrep.2020.108185

12. Kramer, A., Green, J., Pollard, J., & Tugendreich, S. (2013, December 13). *Causal analysis approaches in Ingenuity Pathway analysis*. OUP Academic. https://doi.org/10.1093/bioinformatics/btt703.

13. Langfelder, P., Zhang, B., & Horvath, S. (2007, November 16). *Defining clusters from a hierarchical cluster tree: The dynamic tree cut package for r*. OUP Academic. https://doi.org/10.1093/bioinformatics/btm563.

14. Law, C. W., Chen, Y., Shi, W., & Smyth, G. K. (2014). Voom: Precision weights Unlock linear model analysis tools for RNA-seq read counts. *Genome Biology*, *15*(2). https://doi.org/10.1186/gb-2014-15-2-r29

15. Lei, X., Dong, X., Ma, R., Wang, W., Xiao, X., Tian, Z., Wang, C., Wang, Y., Li, L., Ren, L., Guo, F., Zhao, Z., Zhou, Z., Xiang, Z., & Wang, J. (2020). Activation and evasion of type I interferon responses by SARS-CoV-2. *Nature Communications*, *11*(1). https://doi.org/10.1038/s41467-020-17665-9

16. Liao, Y., Wang, J., Jaehnig, E. J., Shi, Z., & Zhang, B. (2019). WebGestalt 2019: Gene set analysis toolkit with revamped UIs and APIs. *Nucleic Acids Research*, *47*(W1). https://doi.org/10.1093/nar/gkz401

17. Liao, Y., Wang, J., Jaehnig, E. J., Shi, Z., & Zhang, B. (2019, May 22). *WebGestalt 2019: Gene set analysis toolkit with revamped UIs and APIs*. OUP Academic. https://academic.oup.com/nar/article/47/W1/W199/5494758.

18. Liu, S., Cai, X., Wu, J., Cong, Q., Chen, X., Li, T., Du, F., Ren, J., Wu, Y.-T., Grishin, N. V., & Chen, Z. J. (2015). Phosphorylation of innate immune ADAPTOR proteins mavs, sting, and TRIF induces Irf3 activation. *Science*, *347*(6227). https://doi.org/10.1126/science.aaa2630

19. Liu, W., Qiu, X., Song, C., Sun, Y., Meng, C., Liao, Y., Tan, L., Ding, Z., Liu, X., & Ding, C. (2018). Deep Sequencing-Based Transcriptome Profiling Reveals Avian Interferon-Stimulated Genes and Provides Comprehensive Insight Into Newcastle Disease Virus-Induced Host Responses. *Viruses*, *10*(4), 162. https://doi.org/10.3390/v10040162

20. Lokugamage, K. G., Hage, A., de Vries, M., Valero-Jimenez, A. M., Schindewolf, C., Dittmann, M., Rajsbaum, R., & Menachery, V. D. (2020). Type i interferon susceptibility

distinguishes sars-cov-2 from sars-cov. *Journal of Virology*, *94*(23). https://doi.org/10.1128/jvi.01410-20

21. Loutfy, M. R., Blatt, L. M., Siminovitch, K. A., Ward, S., Wolff, B., Lho, H., Pham, D. H., Deif, H., LaMere, E. A., Chang, M., Kain, K. C., Farcas, G. A., Ferguson, P., Latchford, M., Levy, G., Dennis, J. W., Lai, E. K., & Fish, E. N. (2003). Interferon Alfacon-1 Plus Corticosteroids in severe acute respiratory syndrome. *JAMA*, *290*(24), 3222. https://doi.org/10.1001/jama.290.24.3222

22. Mahallawi, W. H., Khabour, O. F., Zhang, Q., Makhdoum, H. M., & Suliman, B. A. (2018). MERS-CoV infection in humans is associated with A pro-inflammatory Th1 and Th17 Cytokine profile. *Cytokine*, *104*, 8–13. https://doi.org/10.1016/j.cyto.2018.01.025

23. Marchiano, S., Hsiang, T.-Y., Higashi, T., Khanna, A., Reinecke, H., Yang, X., Pabon, L., Sniadecki, N. J., Bertero, A., Gale, M., & Murry, C. E. (2020). Sars-cov-2 infects human pluripotent stem cell-derived cardiomyocytes, impairing electrical and mechanical function. https://doi.org/10.1101/2020.08.30.274464

24. McWhirter, S. M., Fitzgerald, K. A., Rosains, J., Rowe, D. C., Golenbock, D. T., & Maniatis, T. (2003). Ifn-regulatory factor 3-dependent gene expression is defective in tbk1-deficient mouse embryonic fibroblasts. *Proceedings of the National Academy of Sciences*, *101*(1), 233–238. https://doi.org/10.1073/pnas.2237236100

25. Molaei, S., Dadkhah, M., Asghariazar, V., Karami, C., & Safarzadeh, E. (2021). The immune response and Immune evasion characteristics In Sars-cov, MERS-CoV, And SARS-CoV-2: Vaccine design strategies. *International Immunopharmacology*, *92*, 107051. https://doi.org/10.1016/j.intimp.2020.107051

26. Mu, J., Fang, Y., Yang, Q., Shu, T., Wang, A., Huang, M., Jin, L., Deng, F., Qiu, Y., & Zhou, X. (2020). SARS-CoV-2 n protein antagonizes type I Interferon signaling by suppressing phosphorylation and nuclear translocation of STAT1 and STAT2. *Cell Discovery*, *6*(1). https://doi.org/10.1038/s41421-020-00208-3

27. Oliveros, J.C. (2007) VENNY. An interactive tool for comparing lists with Venn Diagrams. https://bioinfogp.cnb.csic.es/tools/venny/index.html.

28. Pomerantz, J. L., & Baltimore , D. (1999). NF-kappa B activation by a Signaling complex Containing TRAF2, TANK and TBK1, a novel IKK-related kinase. *The EMBO Journal*, *18*(23), 6694–6704. https://doi.org/10.1093/emboj/18.23.6694

29. R Core Team (2021). R: A language and environment for statistical computing. R Foundation for Statistical Computing, Vienna, Austria. URL https://www.R-project.org/

30. Ragab, D., Salah Eldin, H., Taeimah, M., Khattab, R., & Salem, R. (2020). The covid-19 cytokine storm; what we know so far. *Frontiers in Immunology*, *11*. https://doi.org/10.3389/fimmu.2020.01446

31. Ritchie, M. E., Smyth, G. K., Shi, W., Law, C. W., Hu, Y., Wu, D., & Phipson, B. (2015, April 20). *limma powers differential expression analyses for rna-sequencing and microarray studies*. Nucleic acids research. https://pubmed.ncbi.nlm.nih.gov/25605792/.

32. Robinson, M. D., & Oshlack, A. (2010). A scaling Normalization method for differential expression analysis of rna-seq data. *Genome Biology*, *11*(3). https://doi.org/10.1186/gb-2010-11-3-r25

33. Robles, E. F., Mena-Varas, M., Barrio, L., Merino-Cortes, S. V., Balogh, P., Du, M.-Q., Akasaka, T., Parker, A., Roa, S., Panizo, C., Martin-Guerrero, I., Siebert, R., Segura, V., Agirre, X., Macri-Pellizeri, L., Aldaz, B., Vilas-Zornoza, A., Zhang, S., Moody, S., … Martinez-Climent, J. A. (2016). Homeobox nkx2-3 promotes marginal-zone Lymphomagenesis by activating B-cell receptor signalling and shaping Lymphocyte dynamics. *Nature Communications*, *7*(1). https://doi.org/10.1038/ncomms11889

34. Sarasin-Filipowicz, M., Oakeley, E. J., Duong, F. H., Christen, V., Terracciano, L., Filipowicz, W., & Heim, M. H. (2008). Interferon signaling and treatment outcome in chronic hepatitis C. *Proceedings of the National Academy of Sciences*, *105*(19), 7034–7039. https://doi.org/10.1073/pnas.0707882105

35. Schindler, C., Levy, D. E., & Decker, T. (2007). JAK-STAT signaling: FROM INTERFERONS to Cytokines. *Journal of Biological Chemistry*, *282*(28), 20059–20063. https://doi.org/10.1074/jbc.r700016200

36. Shannon P;Markiel A;Ozier O;Baliga NS;Wang JT;Ramage D;Amin N;Schwikowski B;Ideker T; (2003, November). *Cytoscape: A software environment for integrated models of biomolecular interaction networks*. Genome research. https://pubmed.ncbi.nlm.nih.gov/14597658/.

37. Shannon, P., Markiel, A., Ozier, O., Baliga, N. S., Wang, J. T., Ramage, D., Amin, N., Schwikowski, B., & Ideker, T. (2003). Cytoscape: A software environment for Integrated models of biomolecular Interaction Networks. *Genome Research*, *13*(11), 2498–2504. https://doi.org/10.1101/gr.1239303

38. Shibabaw, T., Molla, M. D., Teferi, B., & Ayelign, B. (2020). Role of IFN and complements system: Innate immunity in SARS-CoV-2. *Journal of Inflammation Research*, *Volume 13*, 507–518. https://doi.org/10.2147/jir.s267280

39. Shin, D., Mukherjee, R., Grewe, D., Bojkova, D., Baek, K., Bhattacharya, A., Schulz, L., Widera, M., Mehdipour, A. R., Tascher, G., Geurink, P. P., Wilhelm, A., van der Heden van Noort, G. J., Ovaa, H., Müller, S., Knobeloch, K.-P., Rajalingam, K., Schulman, B. A., Cinatl, J., … Dikic, I. (2020). Papain-like protease regulates sars-cov-2 viral spread and innate immunity. *Nature*, *587*(7835), 657–662. https://doi.org/10.1038/s41586-020-2601-5

40. St. Gelais, C., Roger, J., & Wu, L. (2015). Non-POU domain-containing Octamer-binding protein negatively regulates HIV-1 infection In cd4+t cells. *AIDS Research and Human Retroviruses*, *31*(8), 806–816. https://doi.org/10.1089/aid.2014.0313

41. Thoms, M., Buschauer, R., Ameismeier, M., Koepke, L., Denk, T., Hirschenberger, M., Kratzat, H., Hayn, M., Mackens-Kiani, T., Cheng, J., Straub, J. H., Stürzel, C. M., Fröhlich, T., Berninghausen, O., Becker, T., Kirchhoff, F., Sparrer, K. M., & Beckmann, R. (2020). Structural basis for Translational shutdown and Immune evasion by The NSP1 protein OF SARS-COV-2. *Science*, *369*(6508), 1249–1255. https://doi.org/10.1126/science.abc8665

42. Trouillet-Assant, S., Viel, S., Gaymard, A., Pons, S., Richard, J.-C., Perret, M., Villard, M., Brengel-Pesce, K., Lina, B., Mezidi, M., Bitker, L., Belot, A., Mouton, W., Oriol, G., Compagnon, C., Generenaz, L., Cheynet, V., Ader, F., Becker, A., … Walzer, T. (2020). Type I IFN Immunoprofiling In COVID-19 Patients. *Journal of Allergy and Clinical Immunology*, *146*(1). https://doi.org/10.1016/j.jaci.2020.04.029

43. Wickham H (2016). *ggplot2: Elegant Graphics for Data Analysis*. Springer-Verlag New York. ISBN 978-3-319-24277-4, https://ggplot2.tidyverse.org.

44. World Health Organization. (n.d.). *WHO coronavirus (COVID-19) Dashboard*. World Health Organization. https://covid19.who.int/.

45. Zhou, Q., Chen, V., Shannon, C. P., Wei, X.-S., Xiang, X., Wang, X., Wang, Z.-H., Tebbutt, S. J., Kollmann, T. R., & Fish, E. N. (2020). Interferon-α2b treatment for COVID-19. *Frontiers in Immunology*, *11*. https://doi.org/10.3389/fimmu.2020.01061

Figures.

Fig 1. Baseline ISG signature

A. Heatmap showing all DE genes in the Calu-3 cells after IFN-β treatment. Over-representation analysis was performed on the six clusters defined by hierarchal clustering. **B.** Number of DE genes per time point in each dose in the Calu-3 cells. **C.** Heatmap showing all DE genes in the ACE2/HSAEC1-KT cells after IFN-beta treatment. Over-representation analysis was performed on the six clusters defined by hierarchical clustering. **D.** Number of DE genes per time point in each dose in the ACE2/HSAEC1-KT cells. E. Venn diagram of the DE genes from the Calu-3 and ACE2/HSAEC1-KT cells.

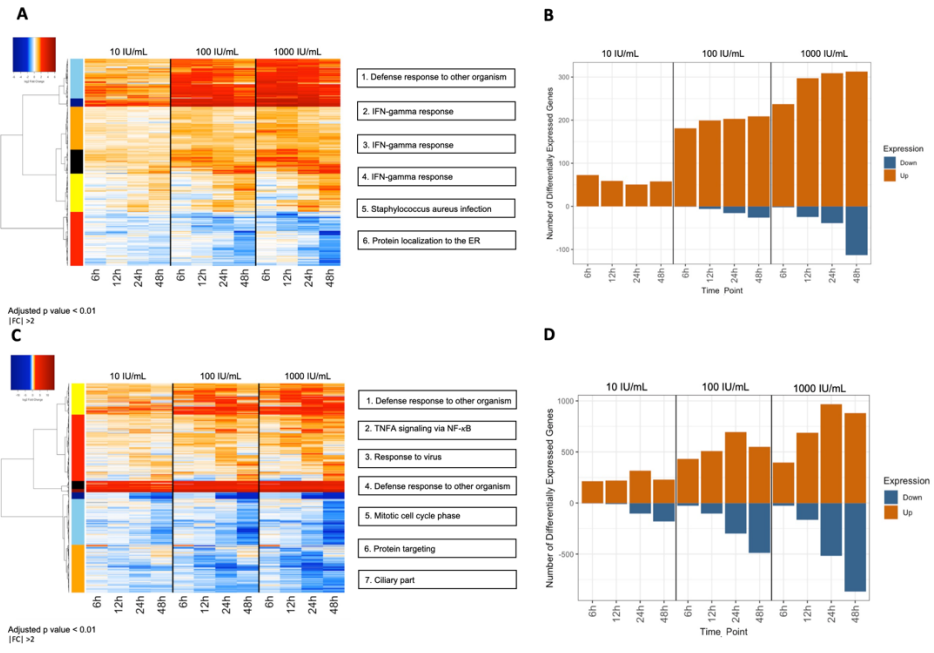

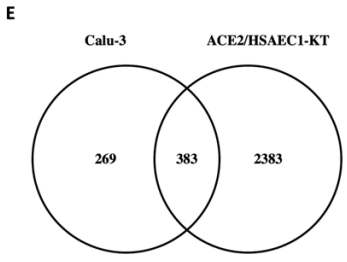

Fig 2. Interaction networks of the top upstream regulators of IFN signaling in Calu-3 cells

A-F. Interaction networks between IRF3, STAT1, NKX2-3, and NONO regulated genes within the Calu-3 DE genes from Cluster 1 (**A**), Cluster 2 (**B**), Cluster 3 (**C**), Cluster 4 (**D**), Cluster 5 (**E**), and Cluster 6 (**F**) of the Calu-3 heatmap in Fig 1. Expression values for each transcription factor represent the $\log_2$(FC) of 1000 IU/mL IFN-β at 6, 12, 24, and 48 hours post treatment from left to right. Arrows indicate direct transcription factor-target interactions (Ingenuity).

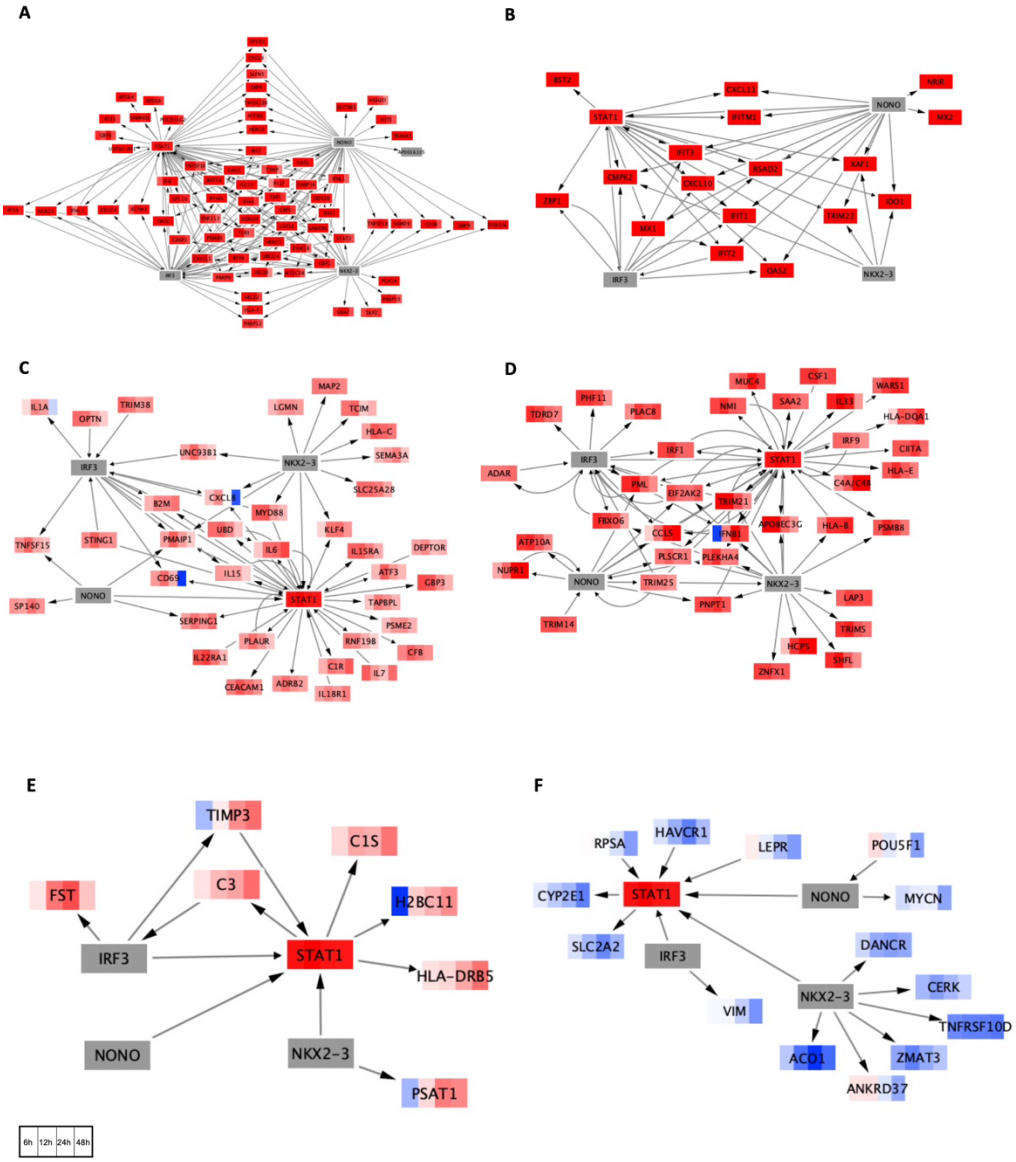

Fig 3. Interaction networks of the top upstream regulators of IFN signaling in ACE2/HSAEC1-KT cells.

A-G. Interaction networks between IRF3, STAT1, NKX2-3, and NONO regulated genes within the ACE2/HSAEC1-KT DE genes from Cluster 1 (**A**), Cluster 2 (**B**), Cluster 3 (**C**), Cluster 4 (**D**), Cluster 5 (**E**), Cluster 6 (**F**), and Cluster 7 (**G**) of the ACE2/HSAEC1-KT heatmap in Fig 1. Expression values for each transcription factor represent the $\log_2$(FC) of 1000 IU/mL IFN at 6, 12, 24, and 48 hours post treatment from left to right. Arrows indicate direct transcription factor-target interactions (Ingenuity).

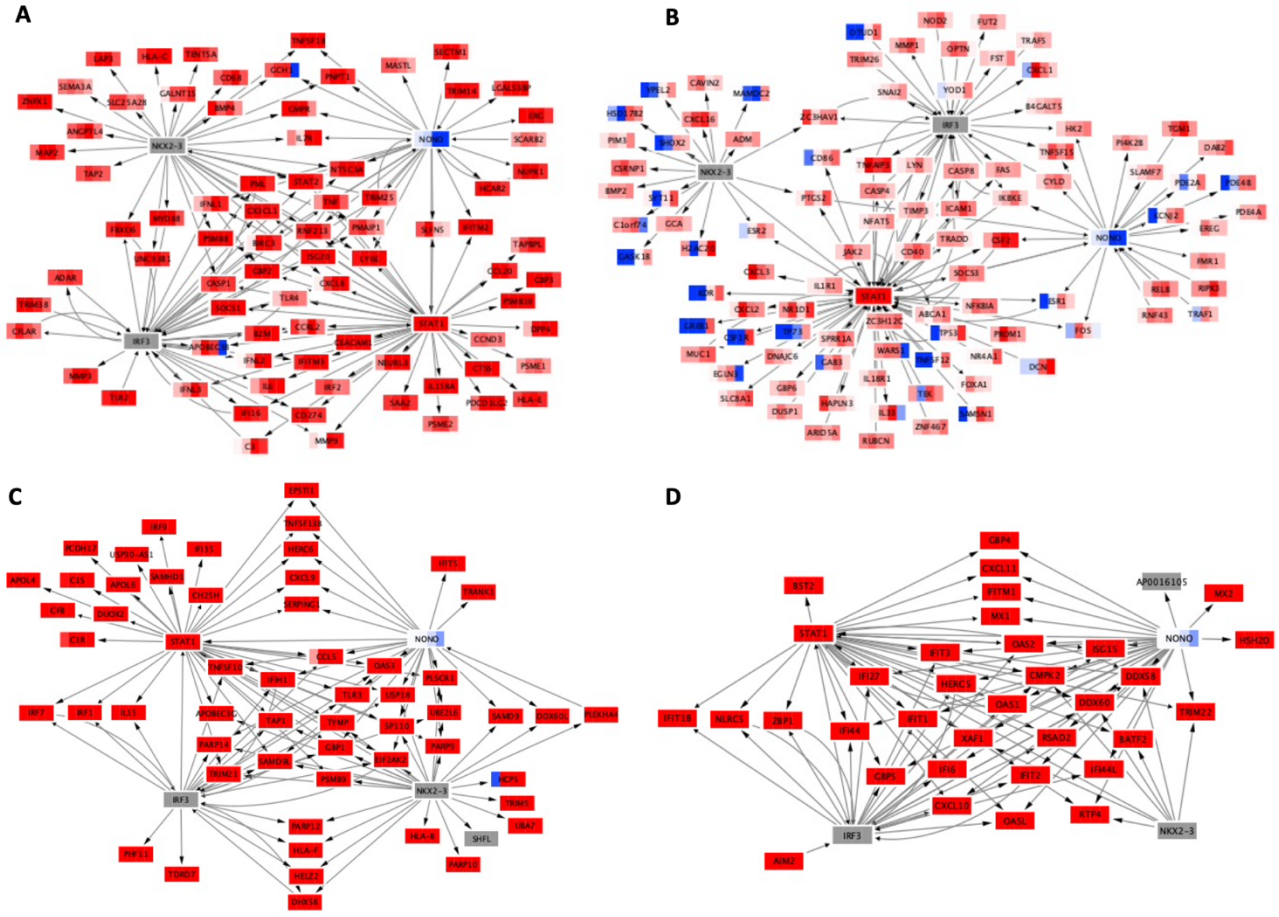

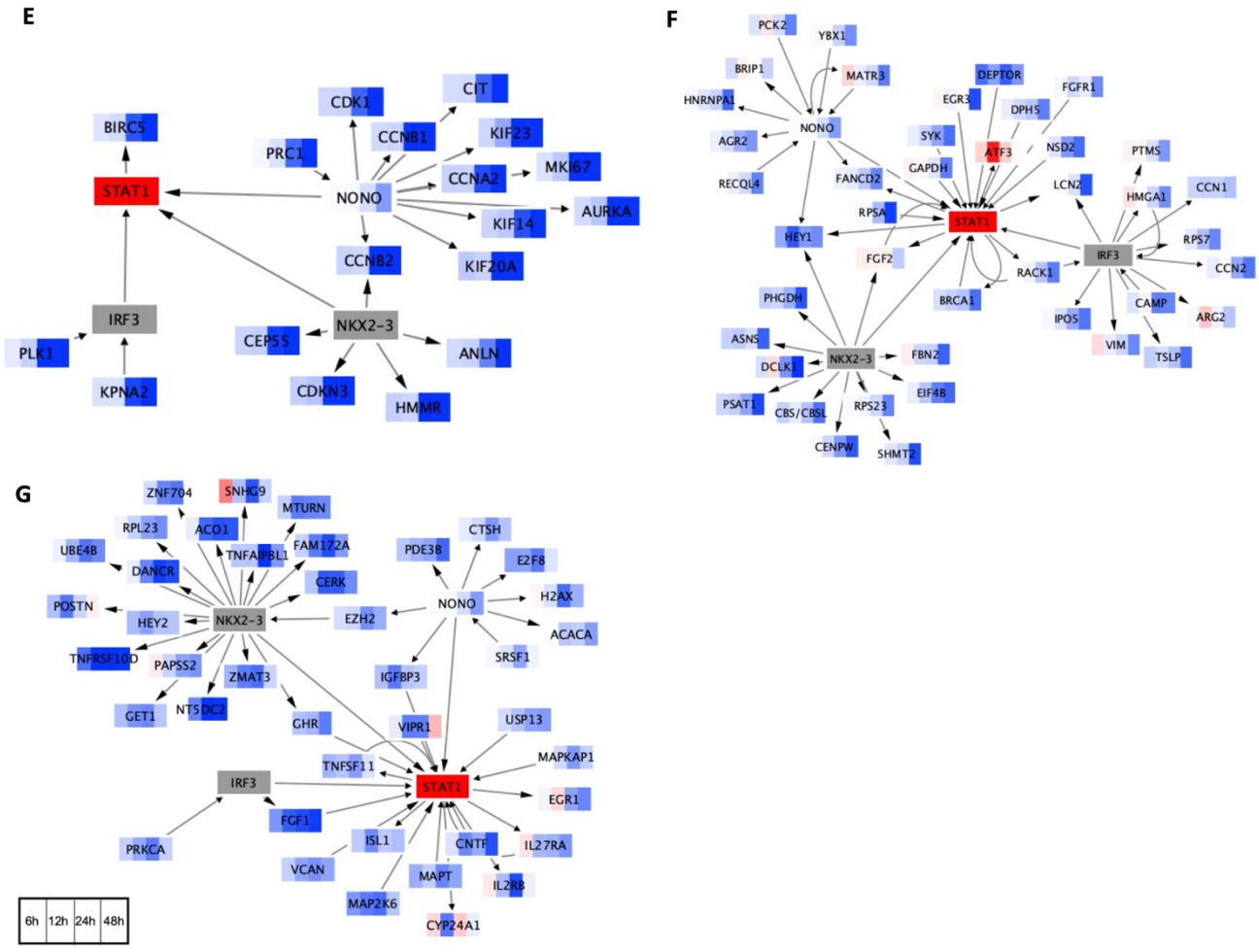
E
BIRC5
CDK1
CIT
CCNB1
KIF23
PRC1
CCNA2
MKI67
STAT1
NONO
AURKA
KIF14
CCNB2
KIF20A
IRF3
NKX2-3
CEP55
ANLN
PLK1
CDKN3
KPNA2
HMMR
F
PCK2
YBX1
BRIP1
MATR3
DEPTOR
FGFR1
HNRNPA1
EGR3
DPH5
NONO
AGR2
SYK
ATF3
NSD2
PTMS
RECQL4
FANCD2
GAPDH
LCN2
HMGA1
CCN1
RPSA
STAT1
HEY1
IRF3
RPS7
FGF2
RACK1
CCN2
PHGDH
BRCA1
CAMP
IPO5
ARG2
ASNS
NKX2-3
FBN2
DCLK1
EIF4B
PSAT1
CBS/CBSL
RPS23
VIM
TSLP
CENPW
SHMT2
G
ZNF704
SNHG9
MTURN
RPL23
ACO1
CTSH
UBE4B
TNFAIP8L1
FAM172A
PDE3B
E2F8
DANCR
CERK
NONO
POSTN
HEY2
NKX2-3
EZH2
H2AX
ACACA
TNFRSF10D
PAPSS2
ZMAT3
SRSF1
IGFBP3
GET1
NT5DC2
GHR
VIPR1
USP13
MAPKAP1
TNFSF11
IRF3
STAT1
EGR1
FGF1
PRKCA
ISL1
CNTF
IL27RA
VCAN
MAPT
IL2RB
MAP2K6
CYP24A1
6h
12h
24h
48h

Fig 4. SARS-CoV-2 induced ISG signature.

A. Heatmap showing all DE genes in the Calu-3 cells after infection with SARS-CoV-2 (MOI:5). Over-representation analysis was performed on the four clusters defined by hierarchal clustering. **B.** Heatmap showing all DE genes in the ACE2/HSAEC1-KT cells after infection with SARS-CoV-2 (MOI:5). Over-representation analysis was performed on the four clusters defined by hierarchical clustering.

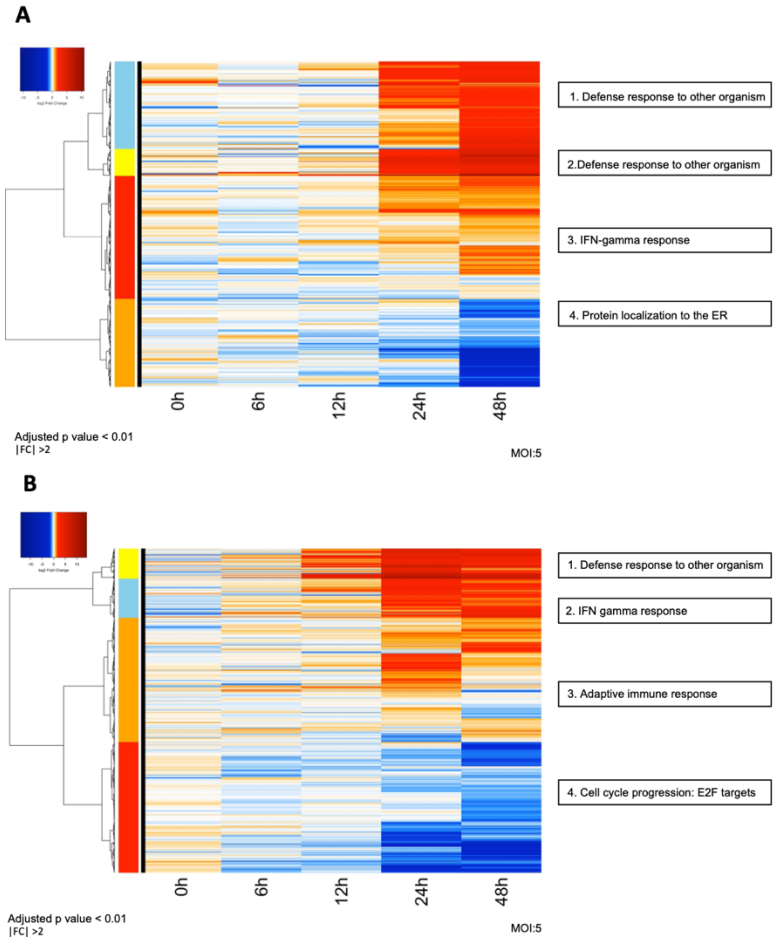

Fig 5. ISGs differentially regulated by IFN treatment before SARS-CoV-2 infection.

A. Heatmap showing all DDE genes in the Calu-3 cells. Three clusters were defined using hierarchical clustering. Over-representation analysis was performed on the three clusters defined by hierarchal clustering. **B.** Heatmap showing all DDE genes in the ACE2/HSAEC1-KT cells. Over-representation analysis was performed on the four clusters defined by hierarchal clustering

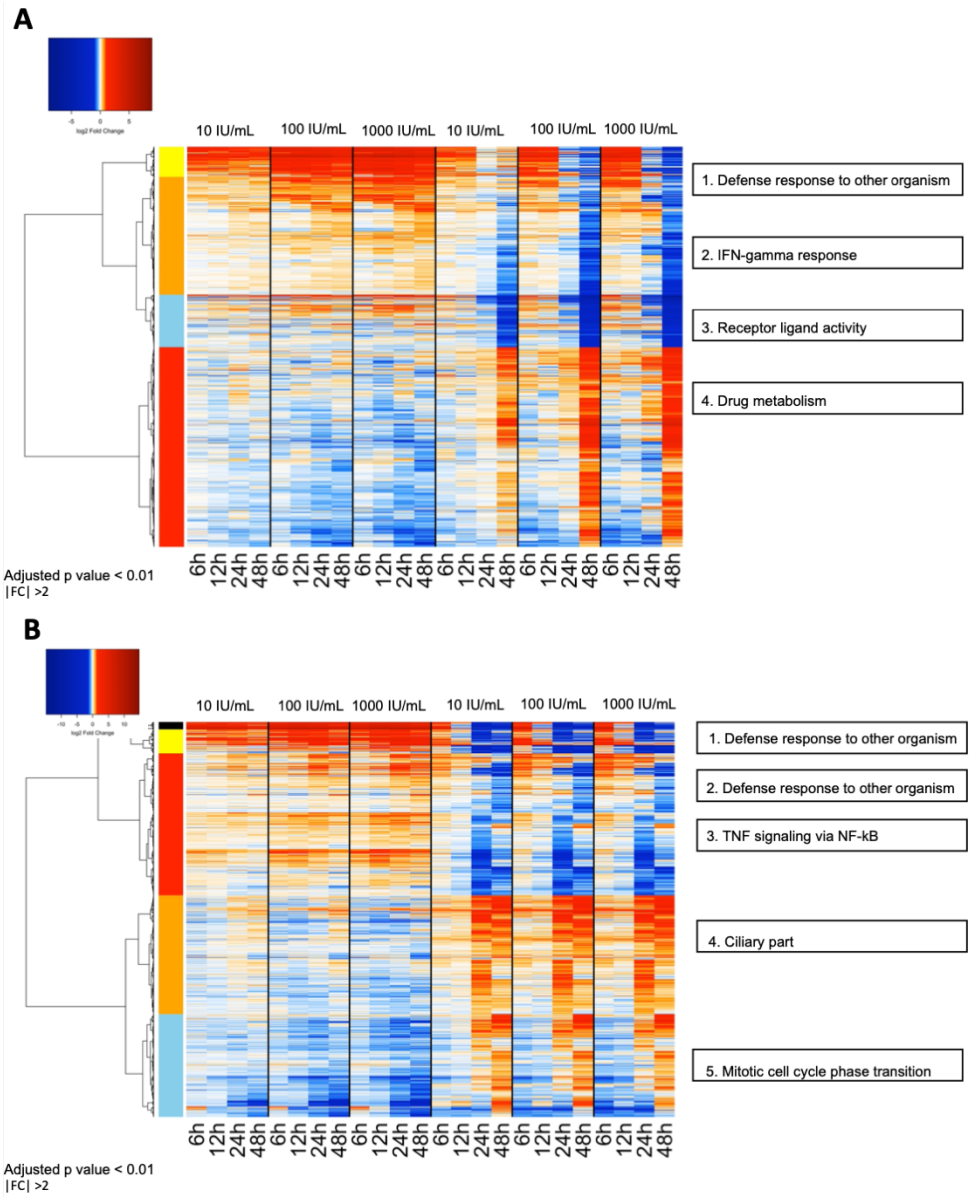

Fig 6. ISGs differentially regulated in response to IFN-β treatment post SARS-CoV-2 infection.

A. Heatmap showing all DDE genes in the Calu-3 cells. Three clusters were defined using hierarchical clustering. Over-representation analysis was performed on the three clusters defined by hierarchal clustering. **B**. Heatmap showing all DDE genes in the ACE2/HSAEC1-KT cells. Over-representation analysis was performed on the four clusters defined by hierarchal clustering

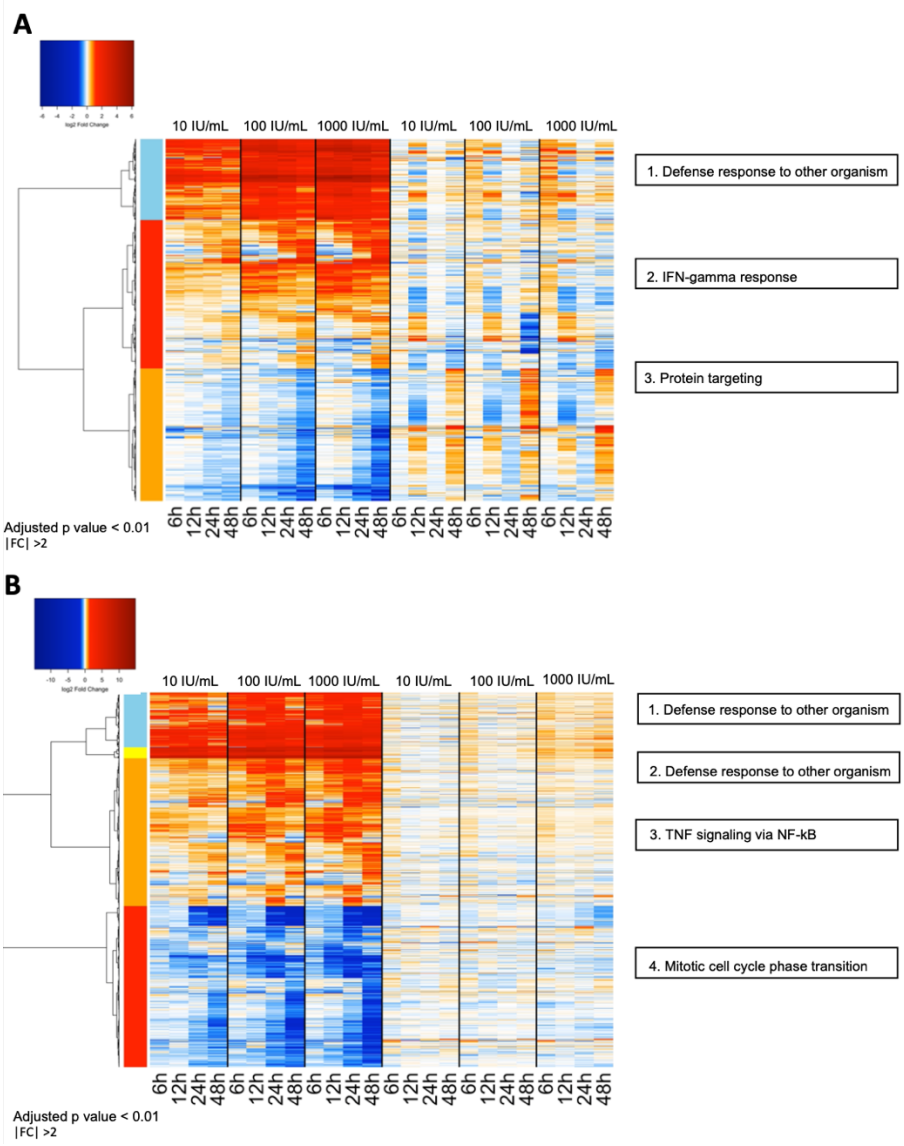

Fig 7. SARS-CoV-2 viral load.

A-C. SARS-CoV-2 viral loads across the time points for each treatment group in the Calu-3 cells. **D-F**. SARS-CoV-2 viral loads across the time points for each treatment group in the ACE2/HSAEC1-KT cells.

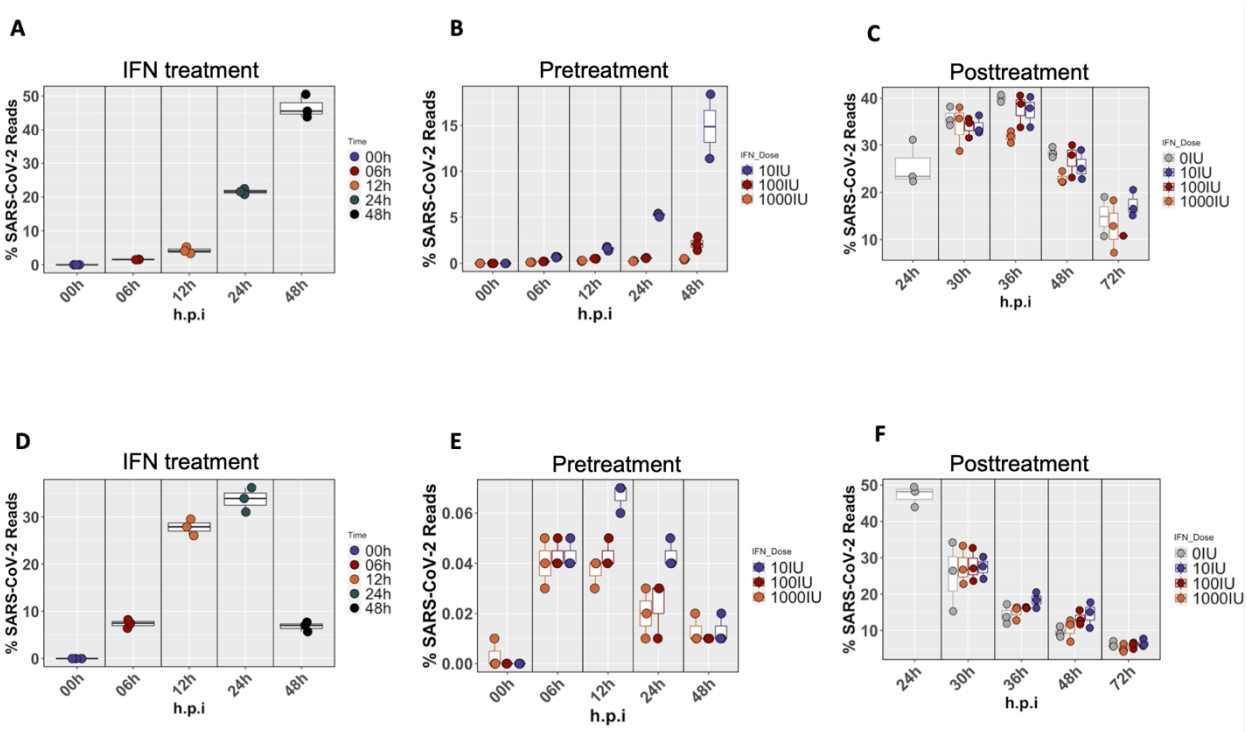

Table 1. Putative antiviral restriction factors identified in the Calu-3 pretreatment samples.

Among the IFN-pretreatment DE genes in the Calu-3 cells, 22 ISGs maintained their expression in the presence of SARS-CoV-2 48 hours post infection.

Gene Symbol	Gene Name	Category	Description
NRIR	Negative regulator of interferon response	RNA gene	Negative regulator of the IFN response
XAF1	XIAP Associated Factor 1	Protein Coding	Counteracts the inhibitory effect of a member of the IAP family
AP001610.1	Novel transcript	RNA gene	lncRNA
OR52K3P	Olfactory Receptor Family 52 Subfamily K Member 3 Pseudogene	Psuedogene	Interacts with odorant molecules in the nose to trigger smell
IFI44L	Interferon Induced Protein 44 Like	Protein Coding	Low antiviral activity against hepatitis C
TRIM22	Tripartite Motif Containing 22	Protein Coding	Down-regulates transcription from the HIV-1 LTR promoter region
ZBP1	Z-DNA Binding Protein 1	Protein Coding	Binds to foreign DNA and induces the type-I interferon production
MX1	MX Dynamin Like GTPase 1	Protein Coding	Antagonizes the replication of several DNA and RNA viruses
MMP13	Matrix Metallopeptidase 13	Protein Coding	Breakdown of extracellular matrix
MX2	MX Dynamin Like GTPase 2	Protein Coding	IFN induced dynamin-like GTPase with potent antiviral activity against HIV
OAS2	2'-5'-Oligoadenylate Synthetase 2	Protein Coding	Activates Rnase L which results in viral RNA degradation
IFI6	Interferon Alpha Inducible Protein 6	Protein Coding	Inhibiting EGFR signaling pathway required for entry of virus into cells
SLAMF6	SLAM Family Member 6	Protein Coding	SLAM receptors trigger activation and differentiation of immune cells
AC008079.2	Family with sequence similarity 230 member D	RNA gene	lncRNA
CNTN4	Contactin 4	Protein Coding	Mediate cell surface interaction during nervous system development
THSD7B	Thrombospondin Type 1 Domain Containing 7B	Protein Coding	Metabolism of proteins
IL33	Interleukin 33	Protein Coding	Cytokine
GC	GC Vitamin D Binding Protein	Protein Coding	Transports vitamin D and its plasma metabolites to target tissues
HLA-DPB1	Major Histocompatibility Complex, Class II, DP Beta 1	Protein Coding	Presents peptides derived from extracellular proteins
RN7SL834P	RNA, 7SL, Cytoplasmic 834, Pseudogene	Psuedogene	-
CRAT37	Cervical cancer-associated transcript 37	RNA gene	lncRNA
HLA-DQA1	Major Histocompatibility Complex, Class II, DQ Alpha 1	Protein Coding	Presents peptides derived from extracellular proteins
HSD17B14	Hydroxysteroid 17-Beta Dehydrogenase 14	Protein Coding	Metabolism of steroids

Table 2. Putative antiviral restriction factors identified in the ACE2/HSAEC1-KT pretreatment samples.

Among the IFN-pretreatment DE genes in the ACE2/HSAEC1-KT cells, 118 ISGs maintained their expression in the presence of SARS-CoV-2 48 hours post infection.

Symbol ID	Gene Name	Category	Description
DHRS2	Dehydrogenase/Reductase 2	Protein Coding	NAPH-dependent dicarbonyl reductase acitivity
AC139493.2	Novel Transcript	RNA gene	lncRNA
PYHIN1	Pyrin And HIN Domain Family Member 1	Protein Coding	HIN-200 family of IFN inducible proteins
SPINK4	Serine Peptidase Inhibitor Kazal Type 4	Protein Coding	Serine protease inhibitor
FYB1	FYN Binding Protein 1	Protein Coding	Involved in platelet activation and expression of IL2
AL606500.1	RNA gene	RNA gene	lncRNA
CLEC7A	C-Type Lectin Domain Containing 7A	Protein Coding	Necessary for the TLR2-mediated inflammatory response
H1-0	H1.0 Linker Histone	Protein Coding	Replication-independent histone
GBP2	Guanylate Binding Protein 2	Protein Coding	Delivers antimicrobial peptides to autophagolysosomes
DCN	Decorin	Protein Coding	Collagen fibril assembly
SLC2A5	Solute Carrier Family 2 Member 5	Protein Coding	Fructose transporter
CCDC144NL-AS	CCDC144NL Antisense RNA 1	RNA gene	lncRNA
TMSB4XP1	TMSB4X Pseudogene 1	Pseudogene	Proposed to participate in cytoskeleton organization
APLN	Apelin	Protein Coding	G protein coupled receptor binding; coreceptor for HIV
OLR1	Oxidized Low Density Lipoprotein Receptor 1	Protein Coding	Its association with oxLDL induces the activation of NF-κB
FABP5P11	Fatty Acid Binding Protein 5 Pseudogene 11	Pseudogene	Regulates somitogenesis
SLC5A10	Solute Carrier Family 5 Member 10	Protein Coding	Sodium/glucose transporter
ADH5P4	ADH5 Pseudogene 4	Pseudogene	tRNA splicing
PPIAP19	Peptidylprolyl Isomerase A Pseudogene 19	Pseudogene	NADH dehydrogenase complex assembly
ANXA2P1	Annexin A2 Pseudogene 1	Pseudogene	Proteasome assembly
AC114801.3	Novel Transcript	Pseudogene	-
PGAM4	Phosphoglycerate Mutase Family Member 4	Protein Coding	Glucose metabolism
AC069528.2	-	uncategorized	-
RPL36A	Ribosomal Protein L36a Pseudogene	Pseudogene	Ribosomal component of the 60S subunit
SULT1B1	Sulfotransferase Family 1B Member 1	Protein Coding	Catalyzes the sulfate conjugation of hormones
TENT5A	Terminal Nucleotidyltransferase 5A	Protein Coding	Non-canonical poly(A) RNA polymerase
ADAM28	ADAM Metallopeptidase Domain 28	Protein Coding	Lymphocyte-expressed ADAM protein
RAB19	RAB19, Member RAS Oncogene Family	Protein Coding	GTPase activity
RPL13P6	Ribosomal Protein L13 Pseudogene 6	Pseudogene	Ribosomal small subunit assembly
CLCA4	Chloride Channel Accessory 4	Protein Coding	Mediates calcium-activated chloride conductance
STC1	Stanniocalcin 1	Protein Coding	Homodimeric glycoprotein with autocrine or paracrine functions
LINC00519	Long Intergenic Non-Protein Coding RNA 519	RNA gene	-
CDH10	Cadherin 10	Protein Coding	Calcium ion binding
TMEM266	Transmembrane Protein 266	Protein Coding	Voltage-sensor protein
PPFIA4	PTPRF Interacting Protein Alpha 4	Protein Coding	Disassembly of focal adhesions
CLEC2B	C-Type Lectin Domain Family 2 Member B	Protein Coding	Roles in inflammation and immune response
GPM6A	Glycoprotein M6A	Protein Coding	Differentiation and migration of neuronal stem cells
HCP5	HLA Complex P5 (lncRNA)	RNA gene	lncRNA
GMPR	Guanosine Monophosphate Reductase	Protein Coding	Catalyzes damination of GMP to IMP
CALHM5	Calcium Homeostasis Modulator Family Member 5	Protein Coding	ATP-releasing channel
APOL4	Apolipoprotein L4	Protein Coding	Lipid exchange and transport
BTN3A3	Butyrophilin Subfamily 3 Member A3	Protein Coding	MHC-associated genes
ERG	ETS Transcription Factor ERG	Protein Coding	Key regulators of inflammation
FABP5P1	Fatty Acid Binding Protein 5 Pseudogene 1	Pseudogene	-
CCRL2	C-C Motif Chemokine Receptor Like 2	Protein Coding	Chemokine receptor-like protein
GCNT2	Glucosaminyl (N-Acetyl) Transferase 2 (I Blood Group)	Protein Coding	Formation of blood group I antigen
AC124319.1	Novel Transcript	RNA Gene	lncRNA
PLAAT4	Phospholipase A And Acyltransferase 4	Protein Coding	Retinoid-inducible gene
SELL	Selectin L	Protein Coding	Cell surface adhesion molecule
TAPBPL	TAP Binding Protein Like	Protein Coding	Member of the Ig superfamily associated with antigen processing
AL671277.1	HLA Complex Group 4 Pseudogene 5	Pseudogene	-
RASSF10	Ras Association Domain Family Member 10	Protein Coding	Regulates embryonic neurogenesis
H2BC21	H2B Clustered Histone 21	Protein Coding	Has broad antibacterial activity
PSMB8-AS1	PSMB8 Antisense RNA 1 (Head To Head)	RNA gene	lncRNA
PSME2P2	Proteasome Activator Subunit 2 Pseudogene 2	Pseudogene	DNA deamination
MMP12	Matrix Metallopeptidase 12	Protein Coding	Breakdown of extracellular matrix
MDK	Midkine	Protein Coding	Cctivation of cAMP-dependent PKA and Akt signaling
BTN3A2	Butyrophilin Subfamily 3 Member A2	Protein Coding	Member of immunoglobulin family
PFKFB4	DEPP1 Autophagy Regulator	Protein Coding	Bifunctional kinase/phosphatase

Table 2 continued.

Symbol ID	Gene Name	Category	Description
SIRPB2	Signal Regulatory Protein Beta 2	Protein Coding	Protein tyrosine phosphatase
ROS1	ROS Proto-Oncogene 1, Receptor Tyrosine Kinase	Protein Coding	Receptor tyrosine kinase
STAT5A	Signal Transducer And Activator Of Transcription 5A	Protein Coding	STAT family of TFs
PATL2	PAT1 Homolog 2	Protein Coding	Oocyte-specific RNA-binding protein
DEPP1	DEPP1 Autophagy Regulator	Protein Coding	Protein encodes a t-SNARE that activates ELK1
AC105749.1	-	Uncategorized	-
IL15	Interleukin 15	Protein Coding	Cytokine that regulates T and NK cell activation and proliferation
RPL23AP37	Ribosomal Protein L23a Pseudogene 37	Pseudogene	-
CCR3	C-C Motif Chemokine Receptor 3	Protein Coding	Receptor for C-C type chemokines
CDK18	Cyclin Dependent Kinase 18	Protein Coding	Protein tyrosine kinase activity
CD74	CD74 Molecule	Protein Coding	Chaperone that regulates antigen presentation for immune response
PPP2R2B	Protein Phosphatase 2 Regulatory Subunit Bbeta	Protein Coding	Ser/Thr Phosphatases implicated in negative cell growth
C3	Complement C3	Protein Coding	Activates complement system
AC009133.1	-	RNA Gene	lncRNA
LINC01358	Long Intergenic Non-Protein Coding RNA 1348	RNA gene	lncRNA
NFASC	Neurofascin	Protein Coding	L1 family immunoglobulin cell adhesion molecule
TSPAN33	Tetraspanin 33	Protein Coding	Role in normal erythropoiesis
GJA5	Gap Junction Protein Alpha 5	Protein Coding	Component of gap junctions
EGLN3	Egl-9 Family Hypoxia Inducible Factor 3	Protein Coding	Prolyl hydroxylase
GALM	Galactose Mutarotase	Protein Coding	Important for normal galactose metabolism
C2orf66	Chromosome 2 Open Reading Frame 66	Protein Coding	-
RET	Ret Proto-Oncogene	Protein Coding	MAPK signaling
KRT6C	Keratin 6C	Protein Coding	Filament protein important for structural integrity of cells
ERAP1	Endoplasmic Reticulum Aminopeptidase 1	Protein Coding	Class I MHC mediated antigen processing and presentation
NPAP1L	Nuclear Pore Associated Protein 1 Like	Pseudogene	Nuclear pore-associated protein
ABCD1	ATP Binding Cassette Subfamily D Member 1	Protein Coding	ATP-binding cassette transporters
STARD5	StAR Related Lipid Transfer Domain Containing 5	Protein Coding	Involved in trafficking lipids and cholesterol
MT-TE	Mitochondrially Encoded TRNA-Glu (GAA/G)	RNA Gene	tRNA aminoacylation
APOL3	Apolipoprotein L3	Protein Coding	Lipid transporter activity
AQP9	Aquaporin 9	Protein Coding	Glycerol channel activity
ACSL5	Acyl-CoA Synthetase Long Chain Family Member 5	Protein Coding	Lipid biosyntehsis and fatty acid degradation
AL356056.2	Uncategorized	RNA Gene	ncRNA
HCAR2	Hydroxycarboxylic Acid Receptor 2	Protein Coding	Nicotinic acid receptor activity
HLA-A	Major Histocompatibility Complex, Class I, A	Protein Coding	Presents peptides derived from ER to cytotoxic T cells
MRGPRX3	MAS Related GPR Family Member X3	Protein Coding	Sensory neuron regulation and modulation of pain
ALMS1P1	ALMS1 Pseudogene 1	Pseudogene	-
MOV10	Mov10 RISC Complex RNA Helicase	Protein Coding	Exhibits antiviral activity against dengue virus
TPM3P8	Tropomyosin 3 Pseudogene 8	Pseudogene	-
PDGFRL	Platelet Derived Growth Factor Receptor Like	Protein Coding	Platelet activating factor receptor activity
TEK	TEK Receptor Tyrosine Kinase	Protein Coding	Prevents leakage of proinflammatory plasma proteins from blood vessels
H2BU1	H2B.U Histone 1	Protein Coding	Component of nucleosome
CES3	Carboxylesterase 3	Protein Coding	Metabolizes xenobiotics
C1S	Complement C1s	Protein Coding	Complement pathway
AL139351.3	lncRNA	RNA Gene	-
TNFRSF14	TNF Receptor Superfamily Member 14	Protein Coding	Member of the TNF receptor superfamily.
RN7SL3	RNA Component Of Signal Recognition Particle 7SL3	RNA Gene	Component of the SRP
H2AW	H2A.W Histone	Protein Coding	Component of the nucleosome
HMGCS1	3-Hydroxy-3-Methylglutaryl-CoA Synthase 1	Protein Coding	Protein homodimerization and isomerase activity
PSME2P1	Proteasome Activator Subunit 2 Pseudogene 1	Pseudogene	-
LINC02542	Long Intergenic Non-Protein Coding RNA 2542	RNA gene	lncRNA
SLC16A4	Solute Carrier Family 16 Member 4	Protein Coding	Monocaroxylate transporter
SAA1	Serum Amyloid A1	Protein Coding	Acute phase protein highly expressed in response to inflammation
UBA7	Ubiquitin Like Modifier Activating Enzyme 7	Protein Coding	Member of the E1 uniquitin-activating enzyme family
TMPRSS11D	Transmembrane Serine Protease 11D	Protein Coding	Trypsin-like protease; type II integral membrane protein
APOBEC3F	Apolipoprotein B MRNA Editing Enzyme Catalytic Subunit 3F	Protein Coding	DNA deaminase; antiviral activity against HIV
LGALS3BP	Galectin 3 Binding Protein	Protein Coding	Modulates cell-cell and cell-matrix interactions
HCAR3	Hydroxycarboxylic Acid Receptor 3	Protein Coding	G protein coupled receptor binding activity
CARD16	Caspase Recruitment Domain Family Member 16	Protein Coding	Induces NF-κB activation during pro-inflammatory cytokine response
HLA-C	Major Histocompatibility Complex, Class I, C	Protein Coding	Presents peptides derived from ER to cytotoxic T cells

Table 3. Putative antiviral restriction factors identified in the Calu-3 posttreatment samples.

Among the IFN-posttreatment DE genes, 33 ISGs are inducible by IFN-β (log_2(FC) >0) 72 hours post SARS-CoV-2 infection in the Calu-3 cells.

Gene Symbol	Gene Name	Category	Description
TMEM14B-DT	TMEM14B Divergent Transcript	RNA gene	lncRNA
NACA3P	NACA Family Member 3, Pseudogene	Pseudogene	-
PRORSD1P	Prolyl-TRNA Synthetase Associated Domain Containing 1, Pseudogene	Pseudogene	Aminoacyl-tRNA editing ability
DBI	Diazepam Binding Inhibitor, Acyl-CoA Binding Protein	Protein Coding	Lipid metabolism
AL359232.1	Novel transcript	RNA gene	lncRNA
SNRPF	Small Nuclear Ribonucleoprotein Polypeptide F	Protein Coding	mRNA splicing
PDCD5	Programmed Cell Death 5	Protein Coding	Regulator of DNA damage response and cell cycle control
SNHG6	Small Nucleolar RNA Host Gene 6	RNA gene	lncRNA
CXCL10	C-X-C Motif Chemokine Ligand 10	Protein Coding	Key regulator of the 'cytokine storm' immune response to SARS-CoV-2 infection.
ACOT13	Acyl-CoA Thioesterase 13	Protein Coding	Catalyzes hydrolysis of acyl-CoA
IDO1	Indoleamine 2,3-Dioxygenase 1	Protein Coding	Modulates immune tolerance and prevents autoimmunity
TRIM22	Tripartite Motif Containing 22	Protein Coding	IFN-induced antiviral protein; ubiquitination of viral proteins
GMPR	Guanosine Monophosphate Reductase	Protein Coding	Catalyzes deamination of GMP to IMP
SEC61G	SEC61 Translocon Subunit Gamma	Protein Coding	Involved in protein translocation across ER membrane
RPL26	Ribosomal Protein L26	Protein Coding	Ribosomal protein that is a component of the 60S subunit of the ribosome
CCL20	C-C Motif Chemokine Ligand 20	Protein Coding	Cytokine activity
GOLT1A	Golgi Transport 1A	Protein Coding	Fusion of ER-derived transport vesicles with golgi
DYSF	Dysferlin	Protein Coding	Involved in muscle contraction and Ca++ mediated membrane fusion events
E2F2	E2F Transcription Factor 2	Protein Coding	DNA binding transcription factor activity
WSCD1	WSC Domain Containing 1	Protein Coding	Sulfotransferase activity
ZBP1	Z-DNA Binding Protein 1	Protein Coding	Binds to foreign DNA and induces the type-I interferon production
TBC1D25	TBC1 Domain Family Member 25	Protein Coding	Vesicle-mediated transport
HSPA12A	Heat Shock Protein Family A (Hsp70) Member 12A	Protein Coding	Cellular response to heat stress
RBP5	Retinol Binding Protein 5	Protein Coding	Retinol binding protein highly expressed in the kidney and liver
AKNA	AT-Hook Transcription Factor	Protein Coding	Centrosomal protein that regulates microtubule orgnaization
RNASE4	Ribonuclease A Family Member 4	Protein Coding	Ribonuclease activity
UBD	Ubiquitin D	Protein Coding	Regulates TNF-alpha-induced and LPS-mediated activation of NF-κB
CD38	CD38 Molecule	Protein Coding	Hydrolase activity
IGF2R	Insulin Like Growth Factor 2 Receptor	Protein Coding	Acts as a positive regulator of T-cell coactivation by binding DPP4
CEBPZOS	CEBPZ Opposite Strand	Protein Coding	-
AC017104.5	Novel transcript	RNA gene	lncRNA
GBP4	Guanylate Binding Protein 4	Protein Coding	Induced by IFN to hydrolyze GTP
SYNPO2	Synaptopodin 2	Protein Coding	Actin binding and actin bundling activity important for cell migration

Table 4. Putative antiviral restriction factors identified in the ACE2/HSAEC1-KT posttreatment samples.

Among the IFN-posttreatment DE genes, 14 ISGs are inducible by IFN-β (log_2(FC) >0) 72 hours post SARS-CoV-2 infection in the Calu-3 cells.

Symbol ID	Gene Name	Category	Description
PCDH17	Protocadherin 17	Protein Coding	Establishes specific cell-cell connections in the brain
SLC15A3	Solute Carrier Family 15 Member 3	Protein Coding	Involved in the detection of microbial pathogens by TLRs and NLRs
BATF2	Basic Leucine Zipper ATF-Like Transcription Factor 2	Protein Coding	AP-1 family TF that controls the differentiation of lineage-specific cells in the immune system
GMPR	Guanosine Monophosphate Reductase	Protein Coding	Catalyzes deamination of GMP to GIP
AC083862.1	Novel Transcript, Antisense to C7orf49	RNA gene	lncRNA
PARD3B	Par-3 Family Cell Polarity Regulator Beta	Protein Coding	Asymmetrical cell division and cell polarization processes
CDKN1C	Cyclin Dependent Kinase Inhibitor 1C	Protein Coding	Negative regulator of cell proliferation
RSAD2	Radical S-Adenosyl Methionine Domain Containing 2	Protein Coding	IFN-inducible antiviral protein that belongs to the SAM superfamily of enzymes
IFIT2	Interferon Induced Protein With Tetratricopeptide Repeats 2	Protein Coding	IFN-induced antiviral protein which inhibits expression of viral mRNAs lacking 2'O-methylation of the 5' cap
CXCL10	C-X-C Motif Chemokine Ligand 10	Protein Coding	Key regulator of the 'cytokine storm' immune response to SARS-CoV-2 infection.
CXCL11	C-X-C Motif Chemokine Ligand 11	Protein Coding	Antimicrobial gene of the CXC chemokine superfamily
XAF1	XIAP Associated Factor 1	Protein Coding	Mediates TNFα induced apoptosis
C11orf96	Chromosome 11 Open Reading Frame 96	Protein Coding	-
RNF175	Ring Finger Protein 175	Protein Coding	Ubiquitin protein ligase activity

Supporting Information

Fig S1. Principal component analysis (PCA)

A. PCA performed on the log_2(CPM) values of all expressed genes in the Calu-3 cells. Samples inside the black box were determined to be outliers and were excluded from subsequent analyses.

B. PCA performed on the log_2(CPM) values of all expressed genes in the ACE2/HSAEC1-KT cells.

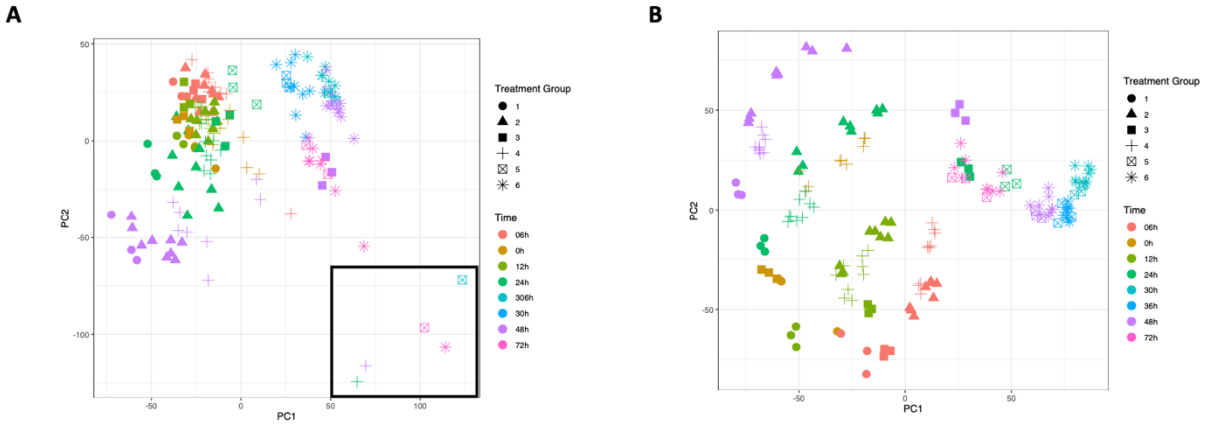

S1 Table. **Gene expression of central transcription factors in interaction networks.**

Gene expression of STAT1, IRF3, NONO, and NKX2-3 transcription factors that are used as central nodes in the interaction networks. Dataset includes log fold-changes from baseline after IFN-β treatment and SARS-CoV-2 infection at all the time points and doses. The (-) indicates genes that had less than 10 raw read counts averaged across all samples and were removed from analyses. The (*) indicates genes that were statistically significantly DE ((FDR)-adjusted $p \leq 0.01$ and absolute log_2(FC) >2).

S2 Table. **IFN-treatment DE genes in Calu-3 cells.**

Baseline ISGs identified from DE analysis in the Calu-3 cells treated with IFN-β. Dataset includes log fold-changes from baseline for all the time points and doses.

S3 Table. **IFN-treatment DE genes in ACE2/HSAEC1-KT cells.**

Baseline ISGs identified from DE analysis in the ACE2/HSAEC1-KT cells treated with IFN-β. Dataset includes log fold-changes from baseline for all the time points and doses.

S4 Table. **IFN-treatment DE genes in Calu-3 and ACE2/HSAEC1-KT cells.**

The shared baseline ISGs identified from DE analysis in both the Calu-3 and ACE2/HSAEC1-KT cells treated with IFN-β.

S5 Table. **IFN-β pretreatment DE genes in the Calu-3 cells.**

Genes identified to have differential expression between the IFN-β pretreatment group and its infected control. The dataset includes log fold-changes from the infected control for all the time points and doses.

S6 Table. **IFN-β pretreatment DE genes in the ACE2/HSAEC1-KT cells.**

Genes identified to have differential expression between the IFN-β pretreatment group and its infected control. The dataset includes log fold-changes from the infected control for all the time points and doses.

S7 Table. **IFN-β pretreatment DDE genes in the Calu-3 cells.**

Dataset includes all DDE genes, defined as genes significantly differentially DE across the time course in any of the three doses, with log fold-changes indicating the difference in DE gene expression in IFN-β treated cells compared to IFN-β pretreated cells.

S8 Table. **IFN-β pretreatment DDE genes in the ACE2/HSAEC1-KT cells.**

Dataset includes all DDE genes, defined as genes significantly differentially DE across the time course in any of the three doses, with log fold-changes indicating the difference in DE gene expression in IFN-β treated cells compared to IFN-β pretreated cells.

S9 Table. **IFN-β posttreatment DE genes in the Calu-3 cells.**

Genes identified to have differential expression between the IFN-β posttreatment group and its infected control. The dataset includes log fold-changes from the infected control for all the time points and doses.

S10 Table. **IFN-β posttreatment DE genes in the ACE2/HSAEC1-KT cells.**

Genes identified to have differential expression between the IFN-β posttreatment group and its infected control. The dataset includes log fold-changes from the infected control for all the time points and doses.

S11 Table. **IFN-β posttreatment DDE genes in the Calu-3 cells.**

Dataset includes all DDE genes, defined as genes significantly differentially DE across the time course in any of the three doses, with log fold-changes indicating the difference in DE gene expression in IFN-β treated cells compared to IFN-β post treated cells.

S12 Table. **IFN-β posttreatment DDE genes in the ACE2/HSAEC1-KT cells.**

Dataset includes all DDE genes, defined as genes significantly differentially DE across the time course in any of the three doses, with log fold-changes indicating the difference in DE gene expression in IFN-β treated cells compared to IFN-β post treated cells.